The Role of Thermal Tides in the Martian Dust Cycle

R. John Wilson

NOAA/Geophysical Fluid Dynamics Laboratory

Princeton, New Jersey

Overview

Hadley Circulation vs Thermal Tides

- Modeling studies have generally focused on simulating major dust storms in the SH summer solstice season due to the expectation that dust is most efficiently lifted and distributed by the Hadley circulation.
- However, the observational record indicates that the dust cycle in most years is dominated by pre- and post-solstice regional dust lifting. In some years major dust storms occurred well before the solstice (Ls=270°), suggesting that the Hadley circulation does not necessarily play the dominant role in dust storm initiation and development.
- It is likely that thermal tides play a more prominent role.

MGCM Simulation of Zonal Mean Surface Stress

Winter Westerlies
+ baroclinic waves

Thermal Tides

Subtropical Jet

Retreating polar cap
boundary

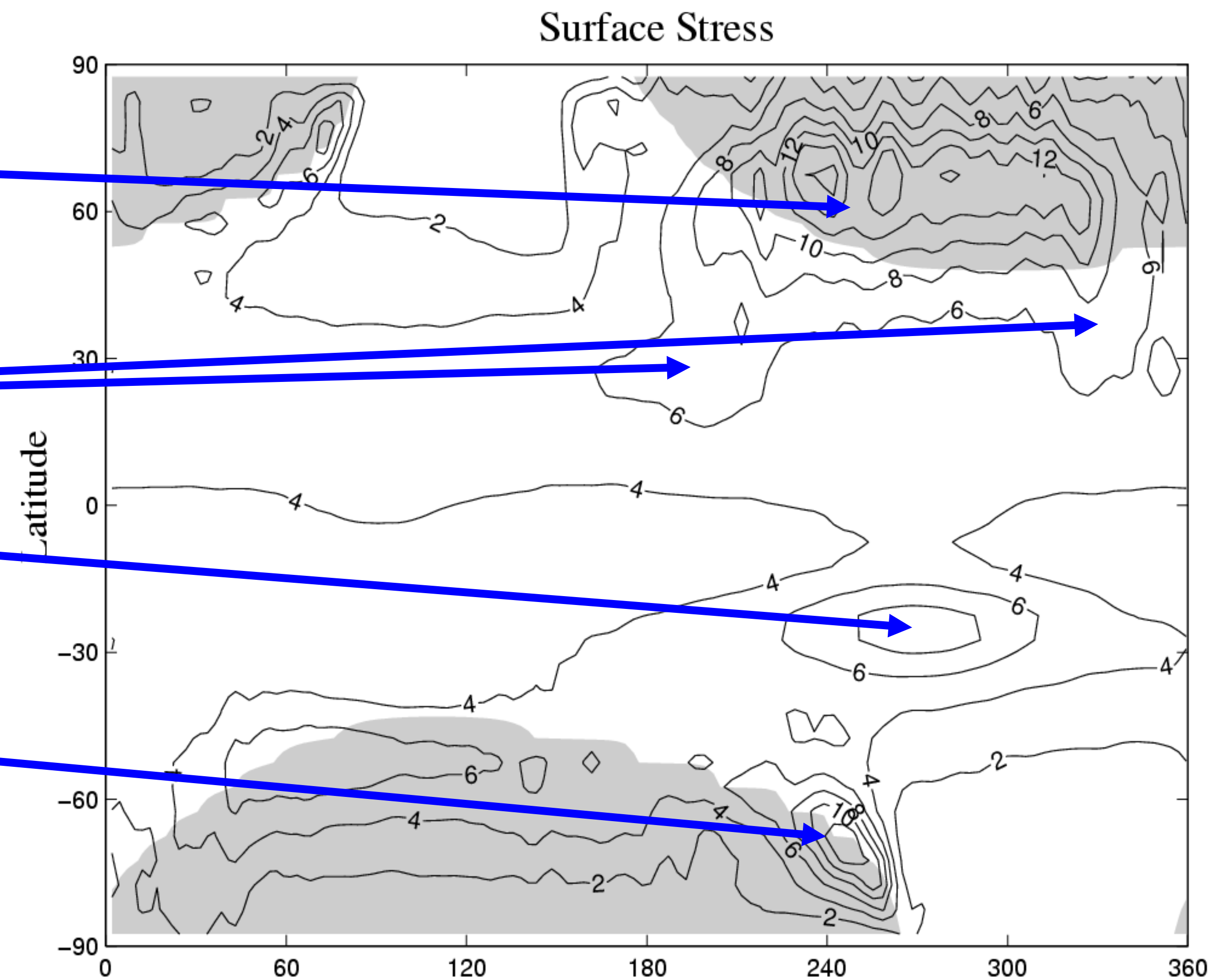

Areocentric Longitude L_s

Polar CO_2 caps are shaded

Units: 10^{-3} Nm^{-2}

Hadley Circulation

Mass Transport Streamfunction

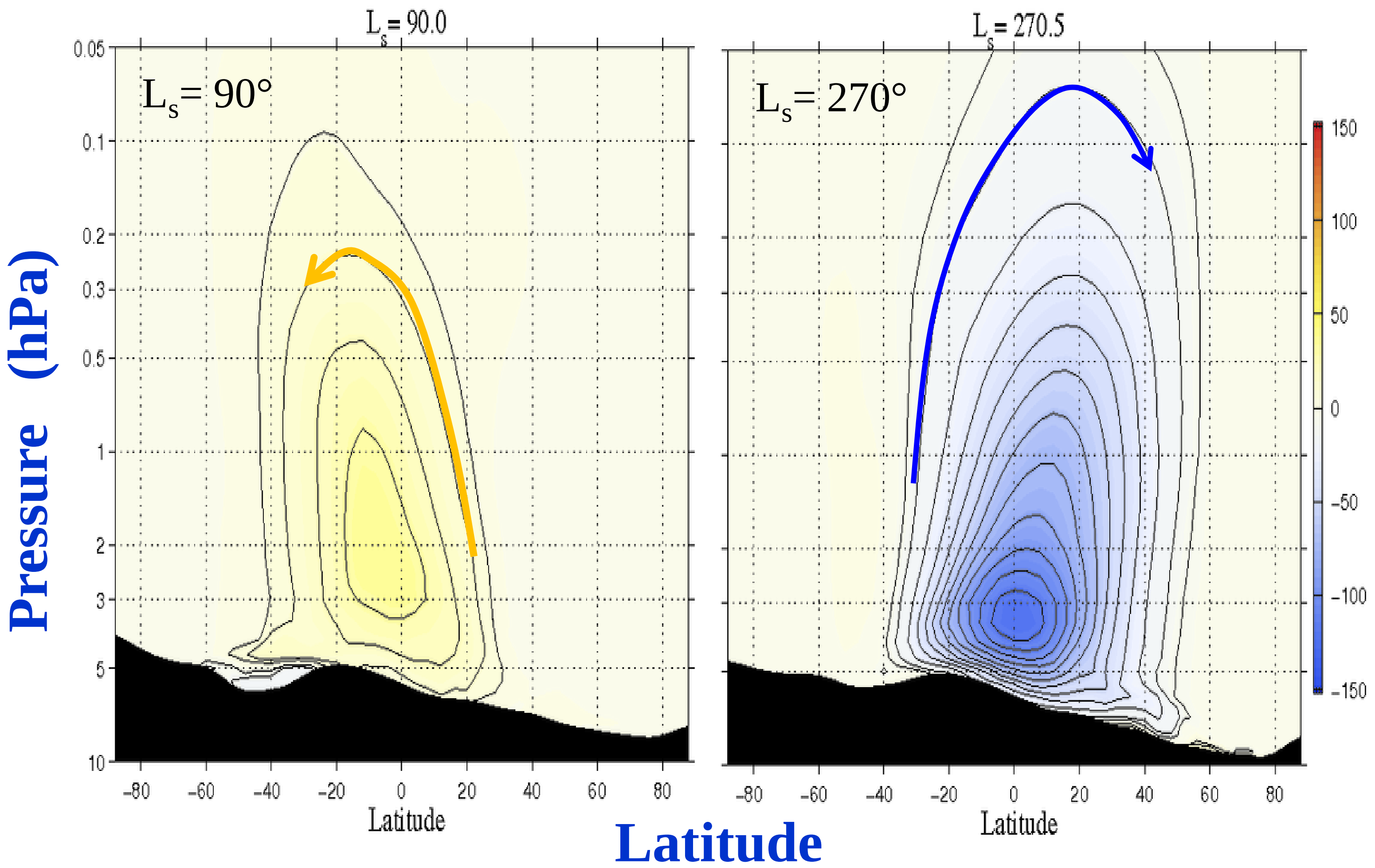

Strong, low-level circulation into the summer hemisphere

Units: 10^8 kg/s

Variation of Hadley Circulation Intensity with Season and Dust Loading

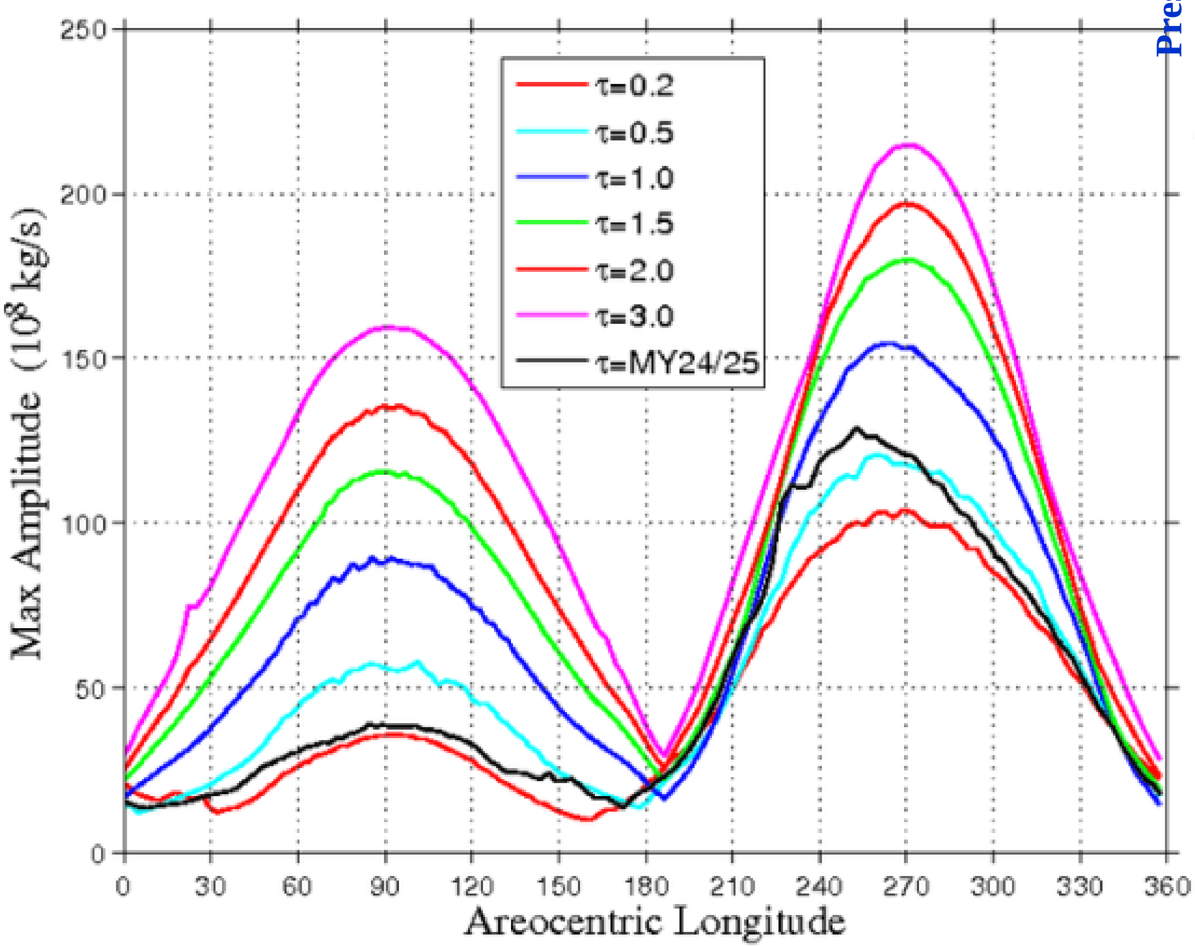

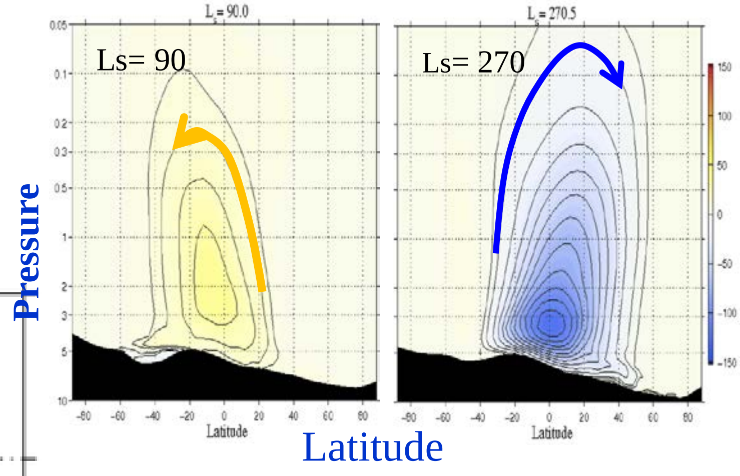

Asymmetry due to zonal mean topography and orbital eccentricity

Strong seasonal variation associated with the migration of the subsolar heating latitude off the equator

Streamfunction: Reanalysis of 4 Years of TES temperatures

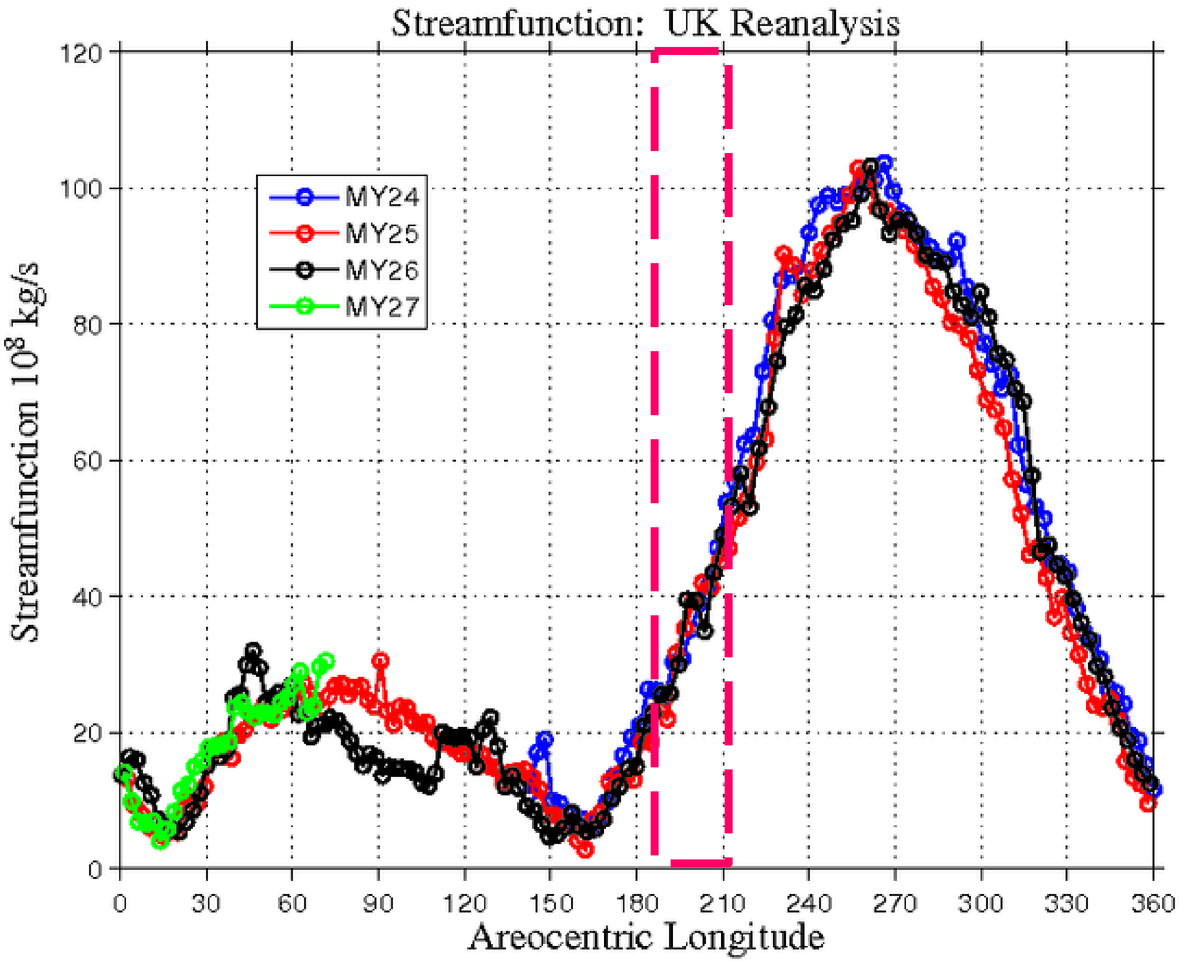

2001 Global Dust storm (MY25, red) had no impact on the Hadley circulation intensity

Diurnal –mean, near-surface winds are not substantially altered; especially the zonal mean component

Tide Surface Pressure and Near-Surface Winds

Global Scale Response to Diurnally-Varying Solar Forcing

Migrating (Sun-synchronous) Tides

Diurnal

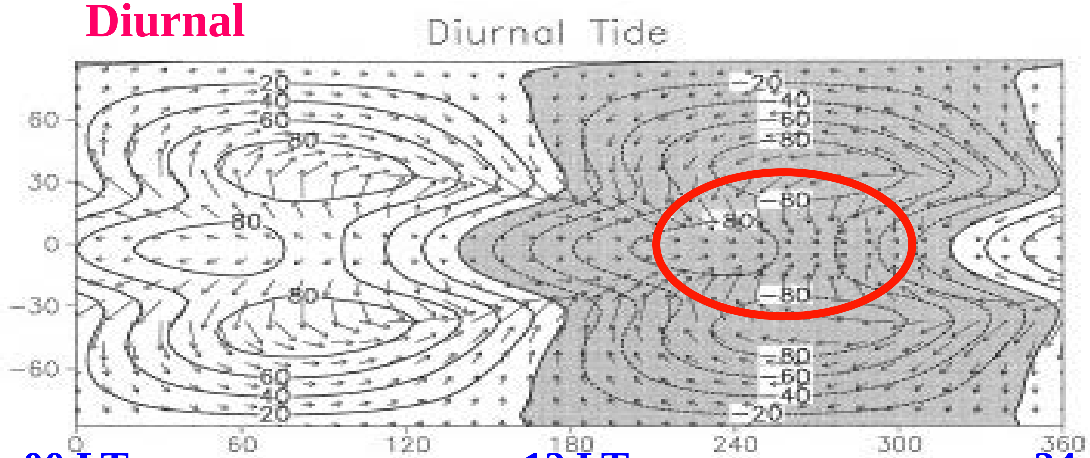

Latitude

00 LT **12 LT** **24**

Winds are strongly divergent/convergent

strong upward motion in the afternoon.

Semidiurnal

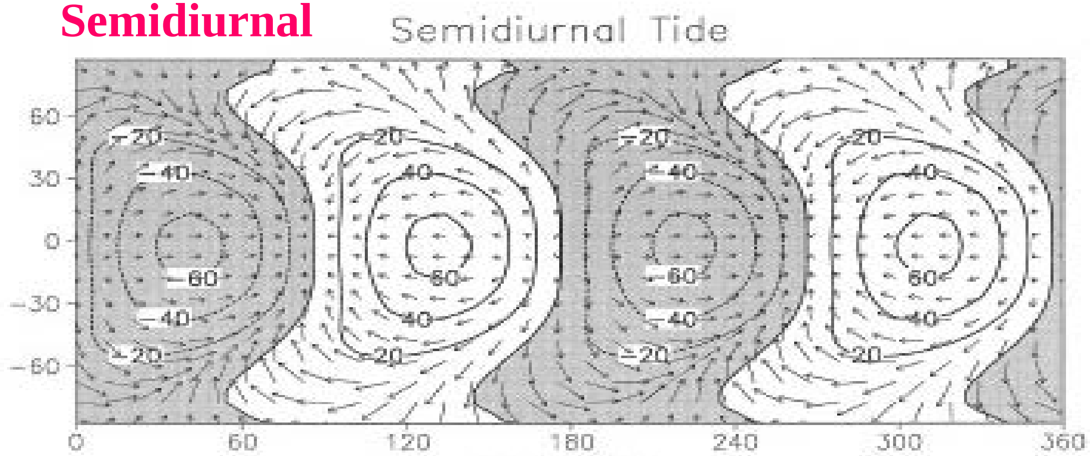

Latitude

00 LT **LOCAL TIME** **24**

S_2 ~ Dust Heating

Zonal Mean Vertical Velocity ώ

380 Pa surface

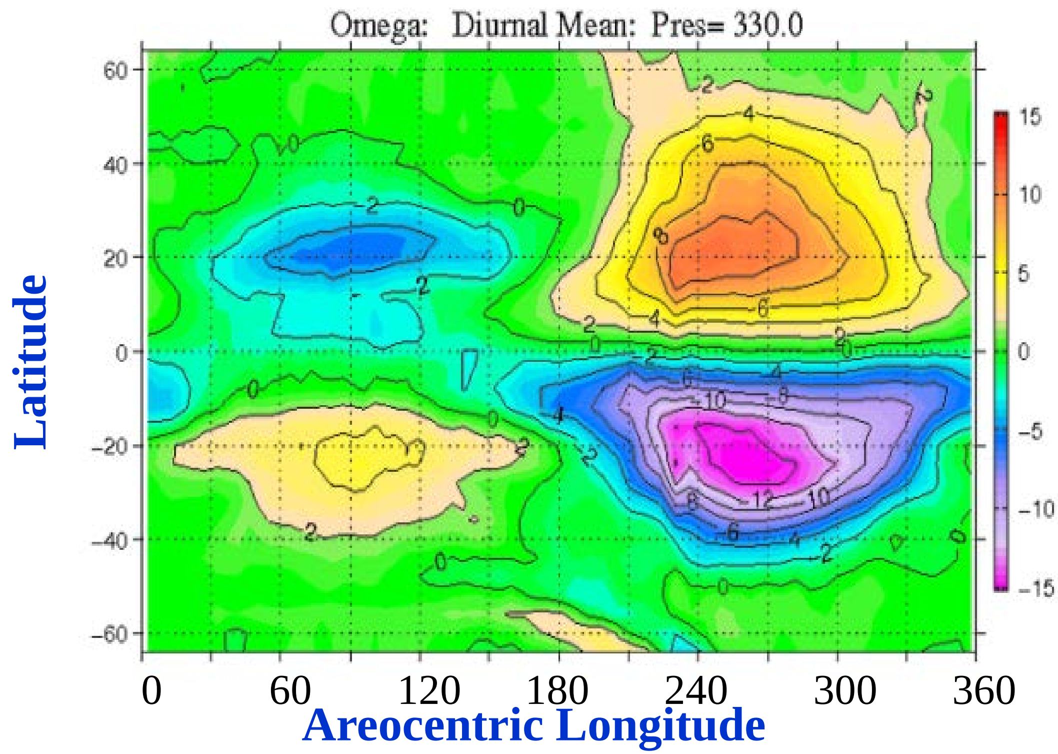

MY24 Simulation

Diurnal Mean ώ

10^4Pa/s

Rising motion in the summer hemisphere

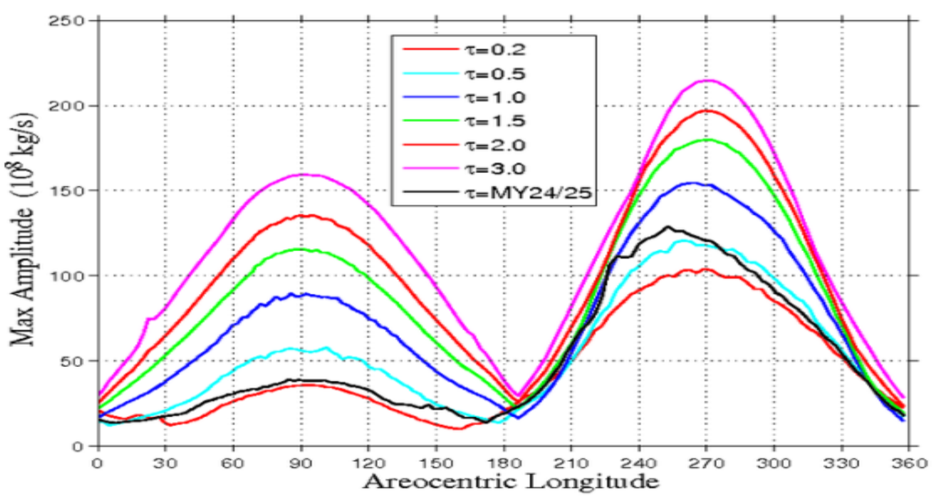

MY24 Simulation

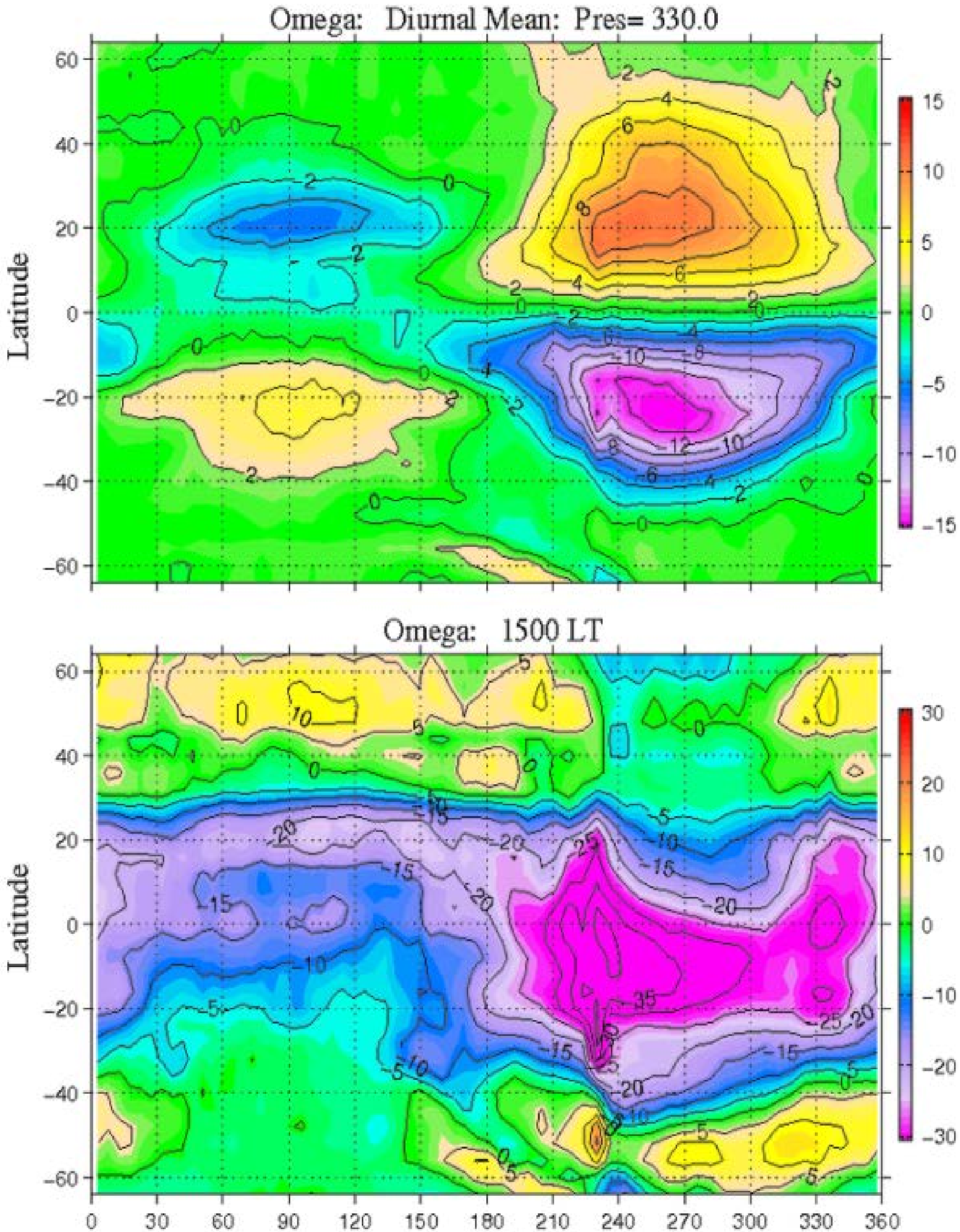

Areocentric Longitude

Diurnal Mean Hadley

-14 x 10^{-4} Pa/s at L_s= 270°

1500 LT Tide Contribution

-40 x 10^{-4} Pa/s at L_s= 235°

Note Change in Color Scale

Tidal Boundary Layer Winds

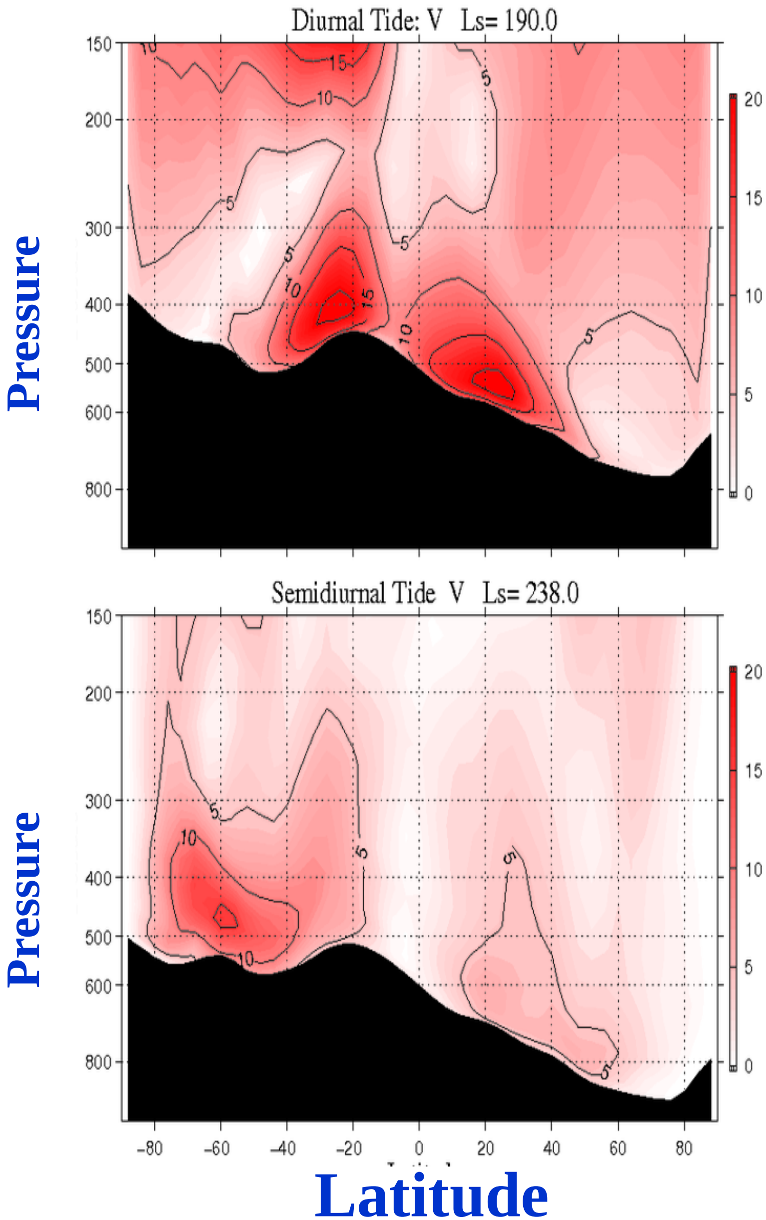

Diurnal Tide Amplitude: V

L_s= 190°

Maximum amplitudes at ~ ±30°

Semidiurnal Amplitude: V

L_s= 238°

contour interval 5 ms^{-1}

Tidal Boundary Layer Winds

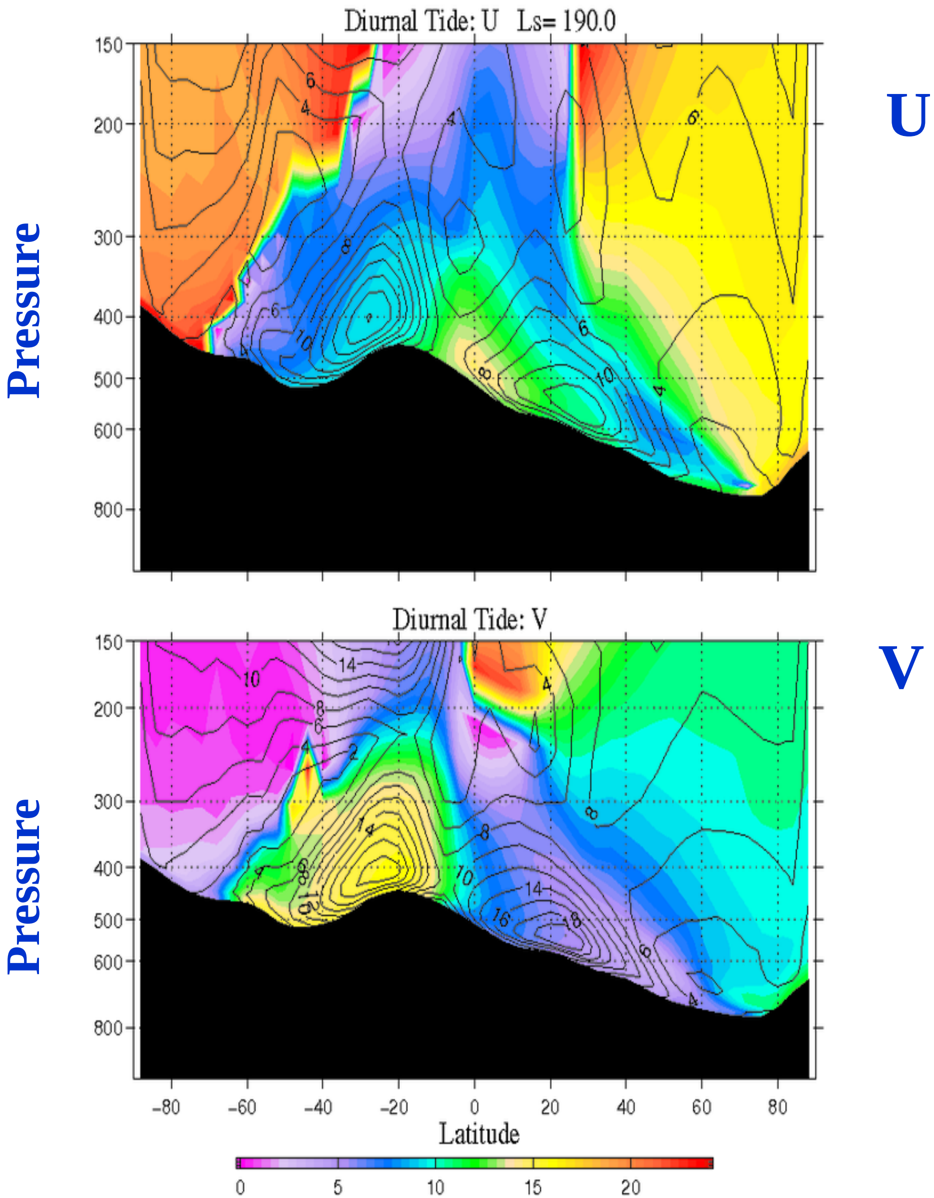

Diurnal Tide Amplitude
contour interval 3 ms^{-1}

Phase (shading 0-24 LT)

Meridional wind is equatorward in late afternoon

Maximum amplitudes at ~ ±30°

Hodograph of Near-Surface Wind

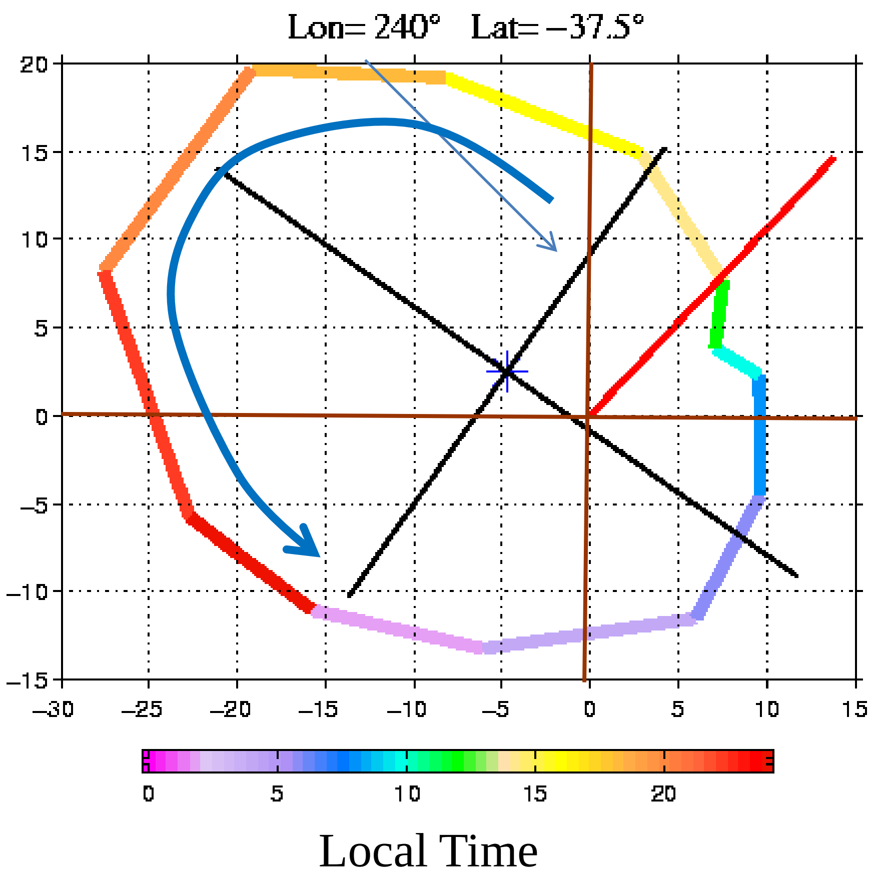

Tide component of wind dominates the diurnal mean

Slope effects less influential away from the surface: tide winds assume the characteristics of the sun-synchronous tide; especially for increased dust loading.

Counterclockwise rotation in the SH

Slope effects can increase the diurnal range of tide winds

Wind Field Analysis: Diurnal Variation of Wind at Selected Locations

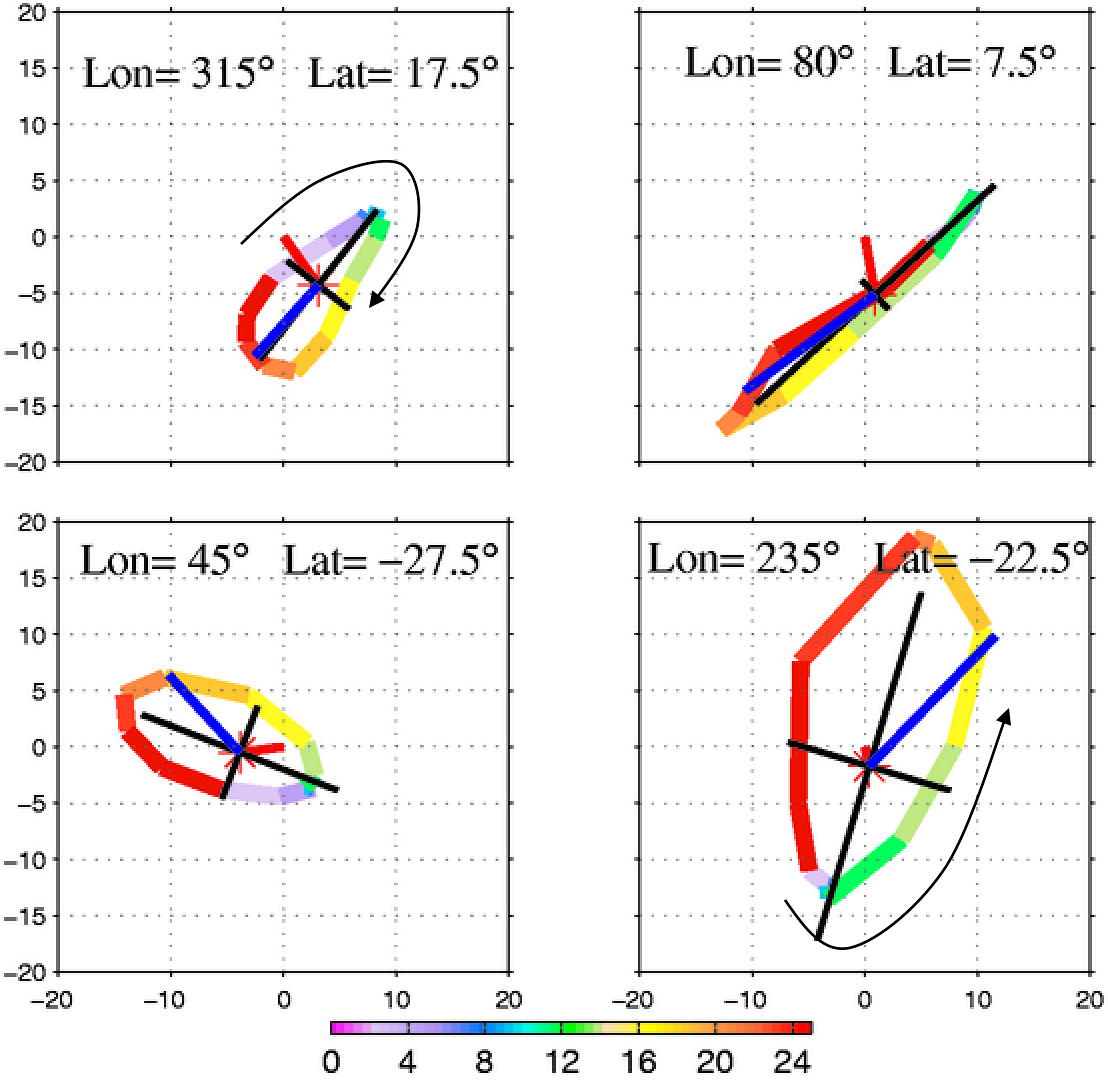

Hodographs: Near surface x and y wind components as functions of local time

Color indicates Local Time:

Clockwise rotation in NH

Counterclockwise in SH

Black axes indicates semimajor and semiminor axis of fitted ellipse (least squares)

Blue line indicates local slope direction

Red line indicates diurnal mean wind

Observed and Simulated Near-Surface Winds

1977b global dust storm

VL1 22N

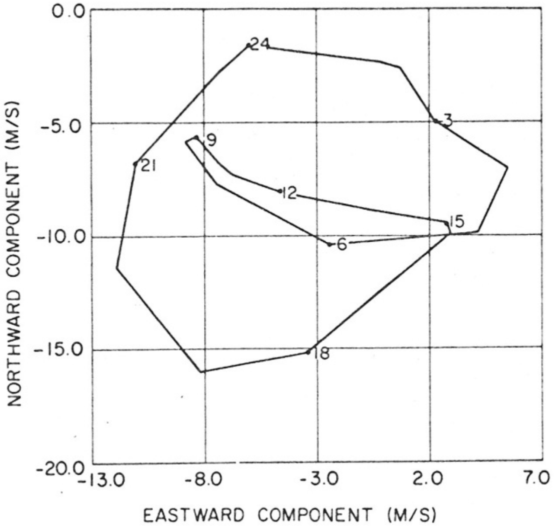

VL2 48N

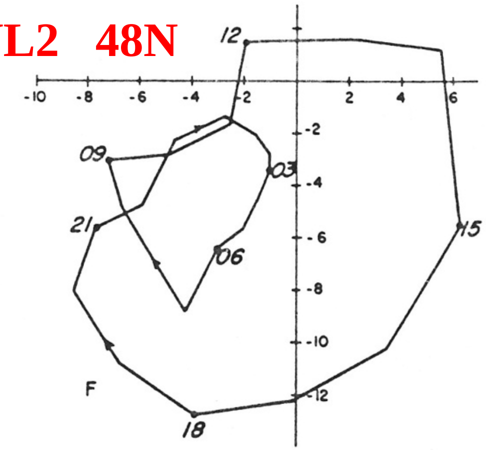

Observed

1.6 m

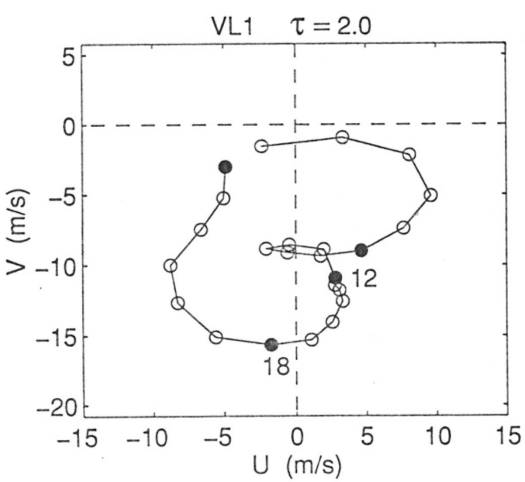

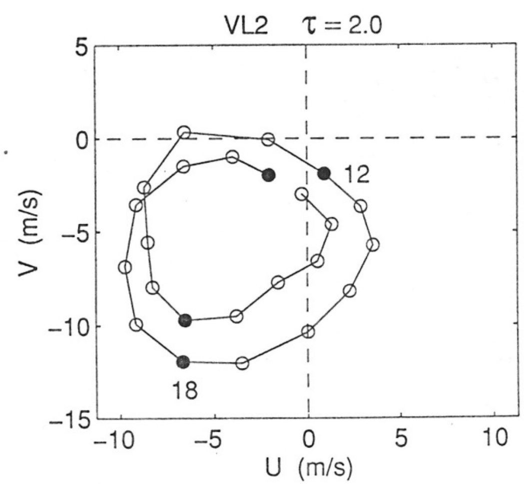

Simulated

40 m

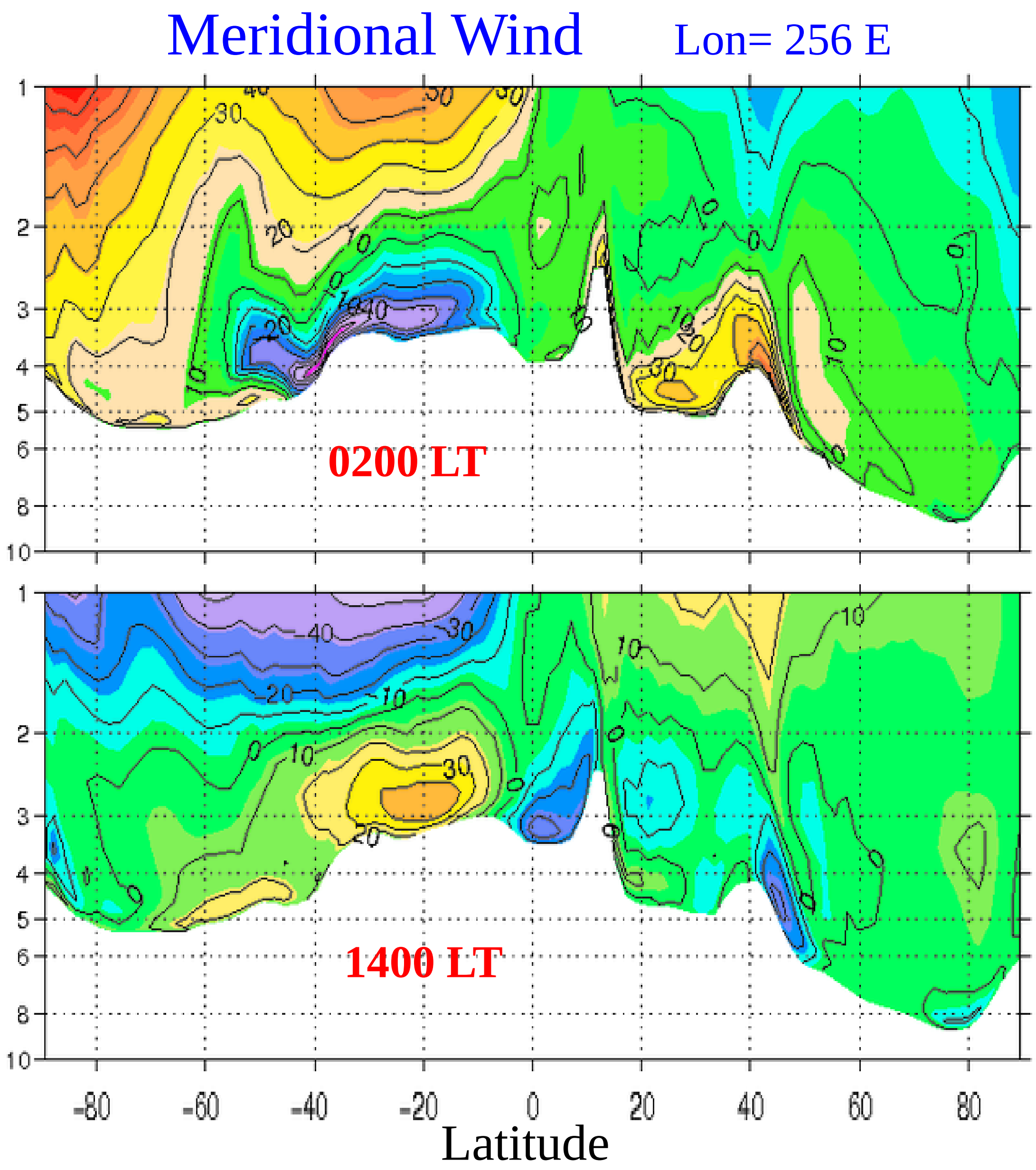

Tide wind + nighttime downslope wind

Low Level Zonal Wind (U)

Fixed Dust simulation $\tau = 0.5$

Diurnal U amplitude

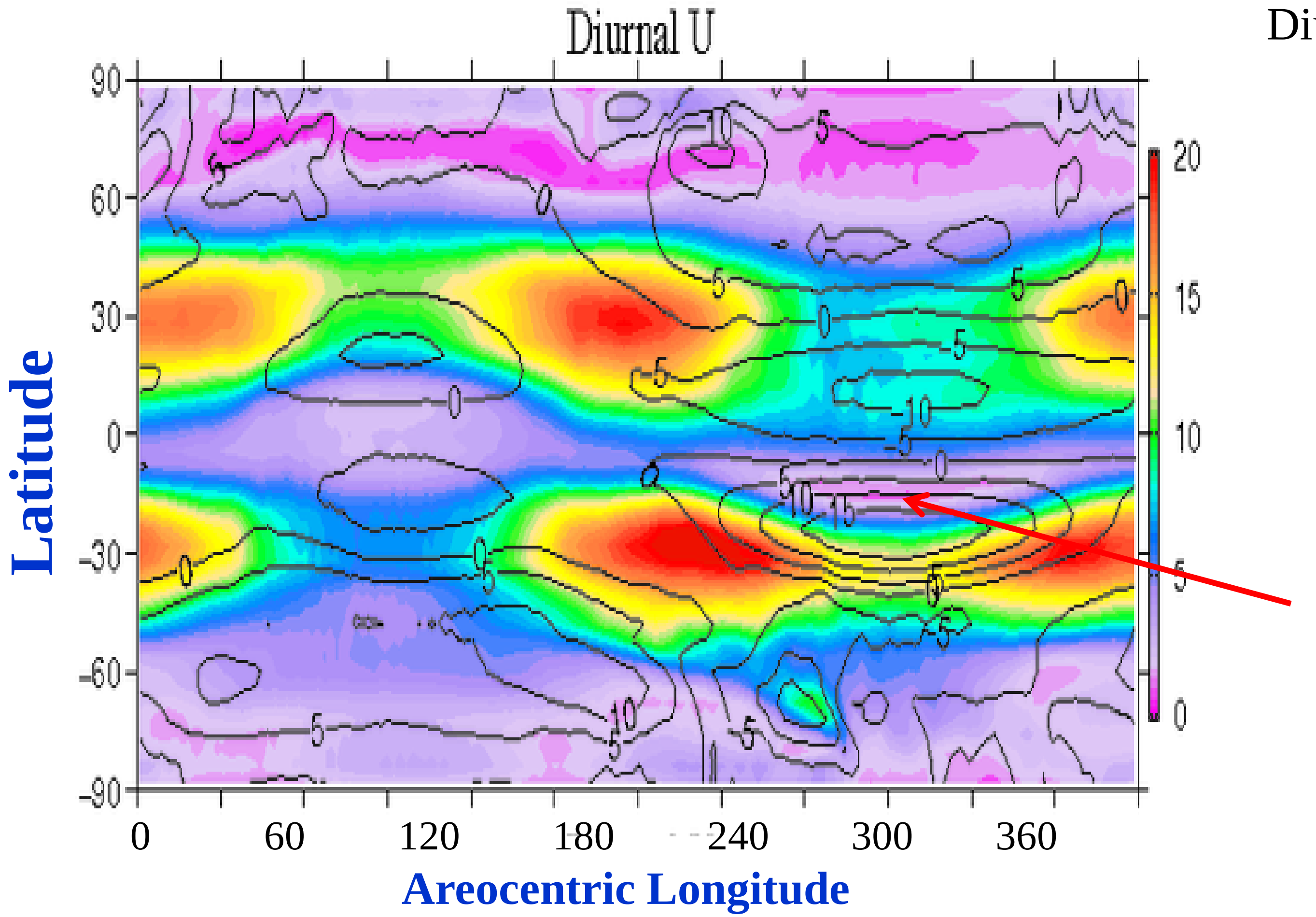

Contours of zonal mean U:
Hadley circulation (5 m/s intervals)

0-20 m/s

Fixed Dust simulation $\tau = 0.5$

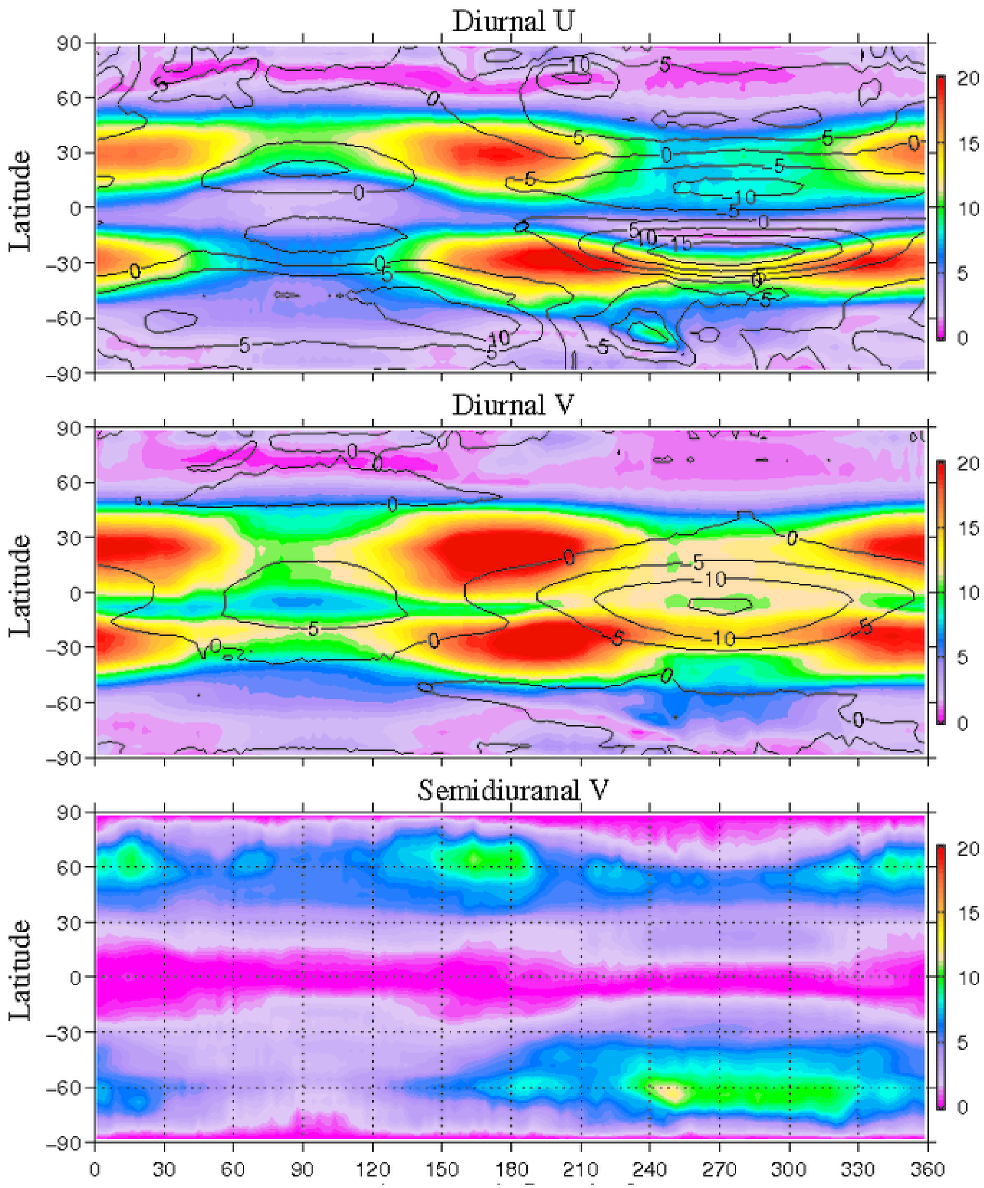

Areocentric Longitude

Diurnal U Amplitude

Diurnal V amplitude

Semidiurnal V amplitude

0-20 m/s

Contours of zonal mean field:
Hadley circulation

MY24 Simulation

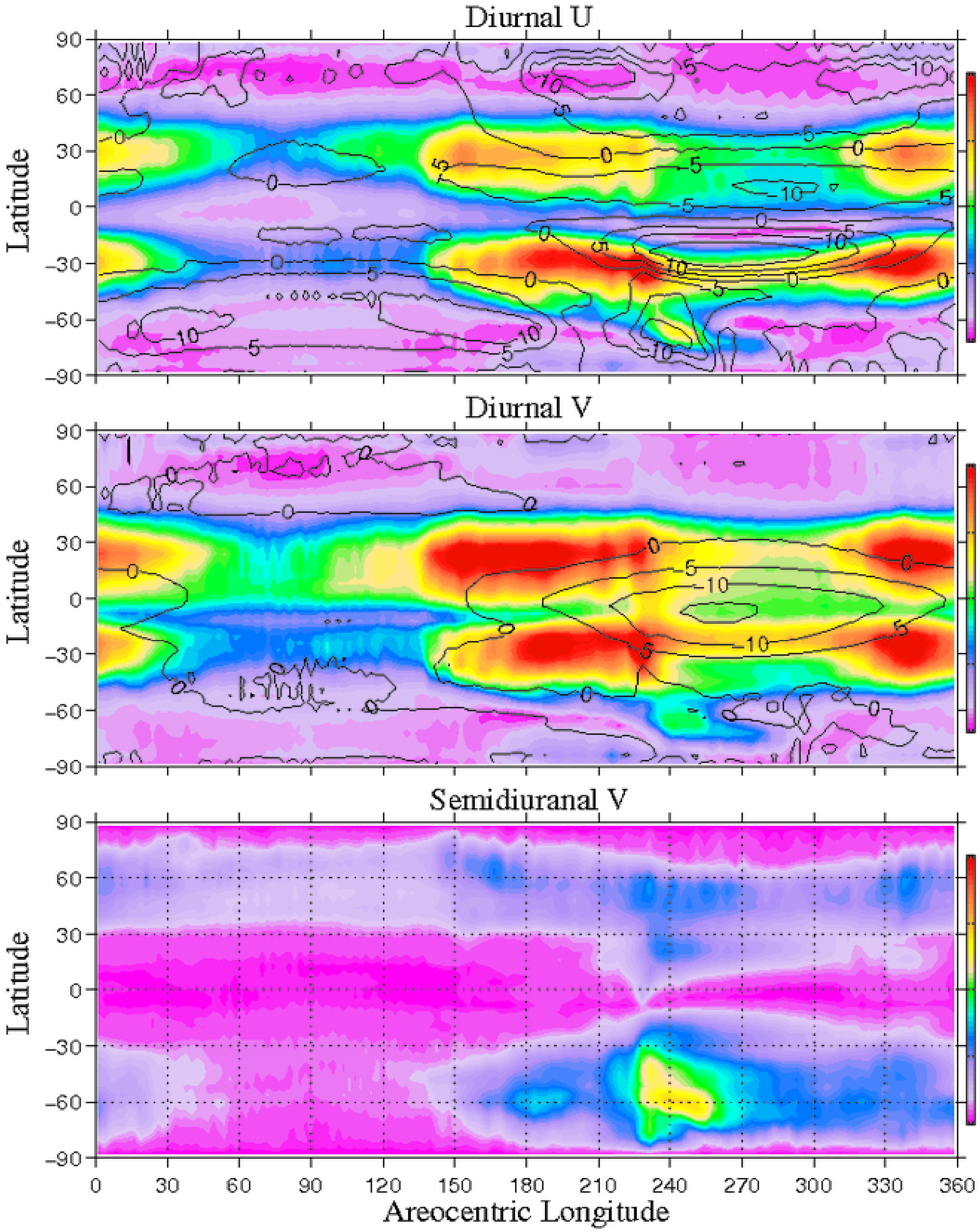

MGCM Simulation of Zonal Mean Surface Stress

Winter Westerlies
+ baroclinic waves

Thermal Tides

Subtropical Jet

Retreating polar cap boundary

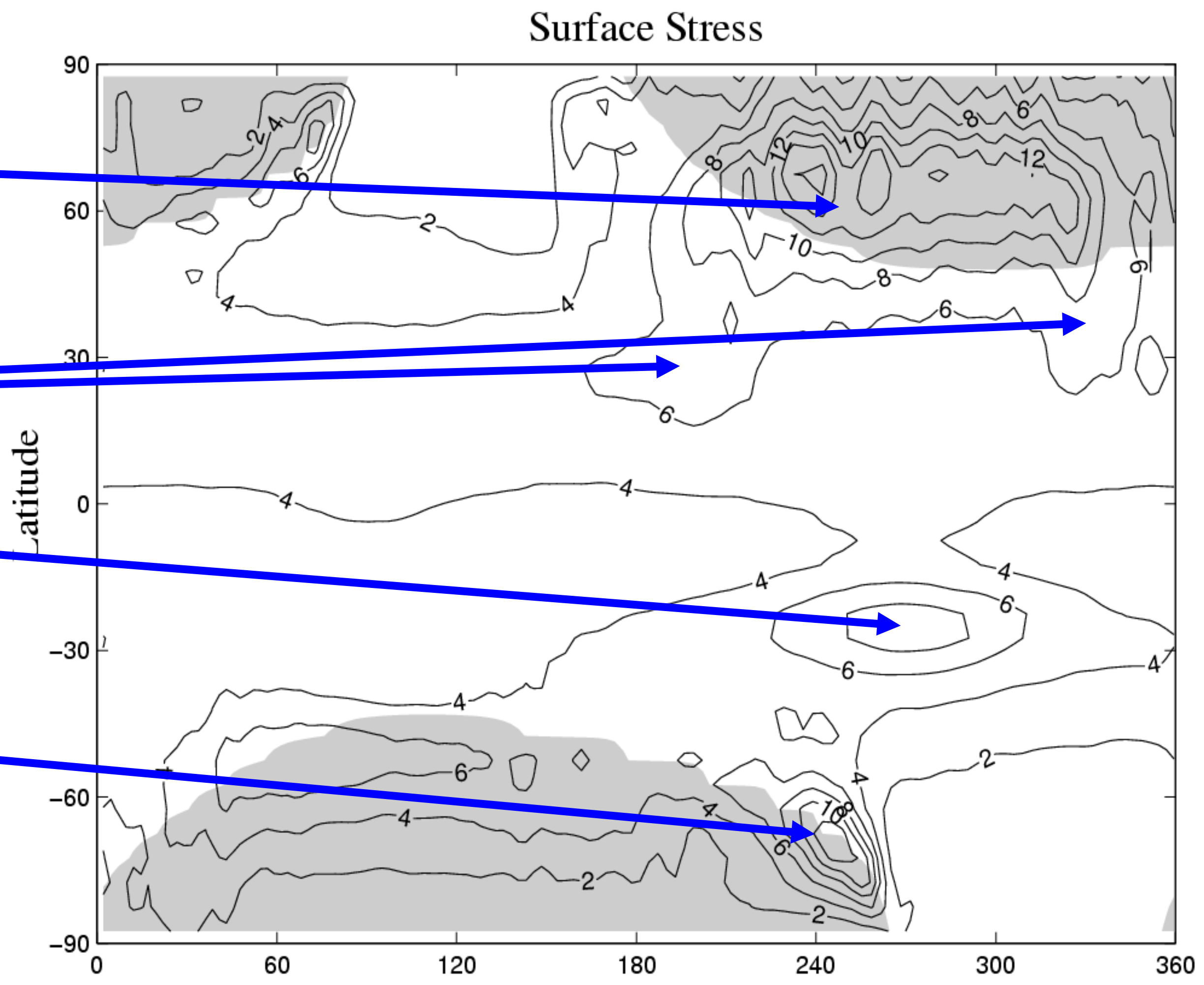

Areocentric Longitude ***L_s***

Polar CO_2 caps are shaded

Units: 10^{-3} Nm^{-2}

Dust, T

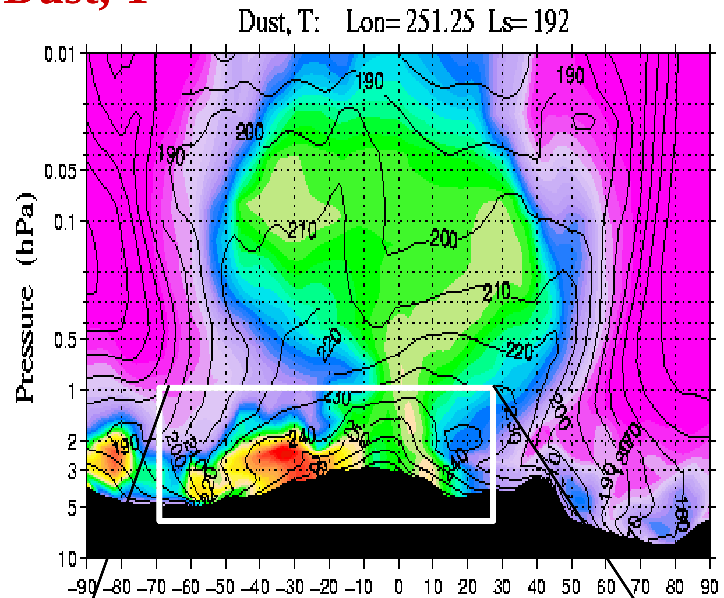

Latitude

Dust, V

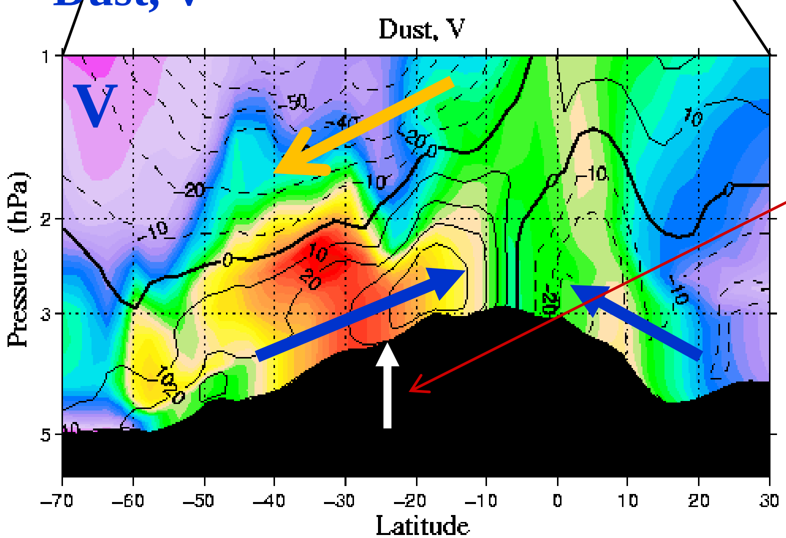

V 10 ms^{-1} intervals

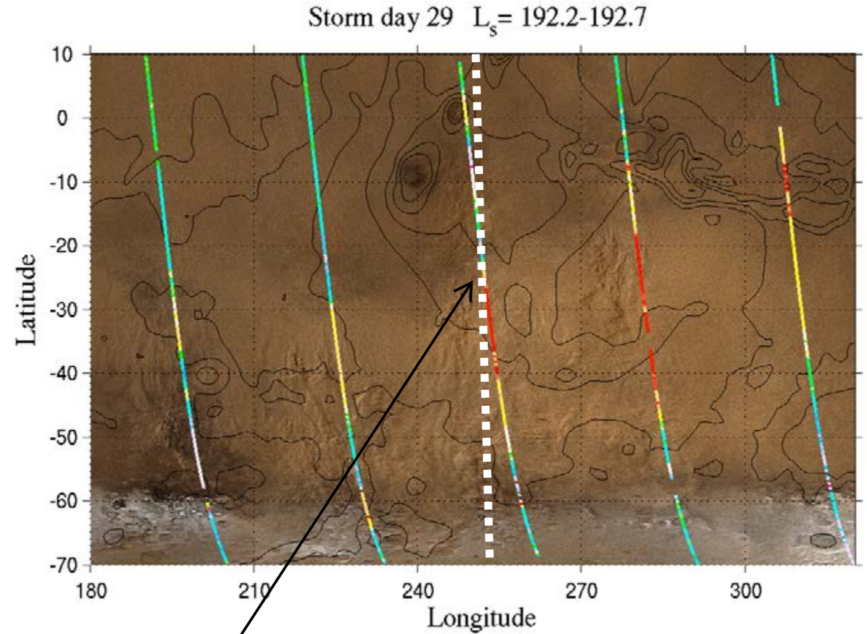

MOC Image

Dust front at 24° S and 250° E

MGCM Simulation: 1400 LT

Meridional Winds dominated by Tides

Summary

• The significant influence of tides on Mars is in notable contrast with the terrestrial atmosphere. **Low level wind variability on Mars is dominated by tides**. Of course, slope wind effects (nonmigrating tides) are a major influence as well.

• The seasonal variation in diurnal tide winds appears to be correlated with the pre- and post-solstice regional storm activity.

• A negative feedback mechanism that can account for dust storm decay is still missing. **The intensity of winds associated with the tides and the Hadley circulation are positively correlated with dust opacity.** The availability of finite mobile surface dust deposits is an obvious possibility for limiting dust lifting in a particular region.

• **Vertical transport of dust out of the boundary layer is evidently dominated by migrating and nonmigrating tides in MGCM simulations**. The Hadley circulation is still the prime circulation element for global scale transport.

• Simulations with 2°x2° spatial resolution are not able to represent small-scale convective plumes that may be important for vertical transport of dust into the free atmosphere.

Earth

Observed Diurnal and Semidiurnal Tide Amplitudes

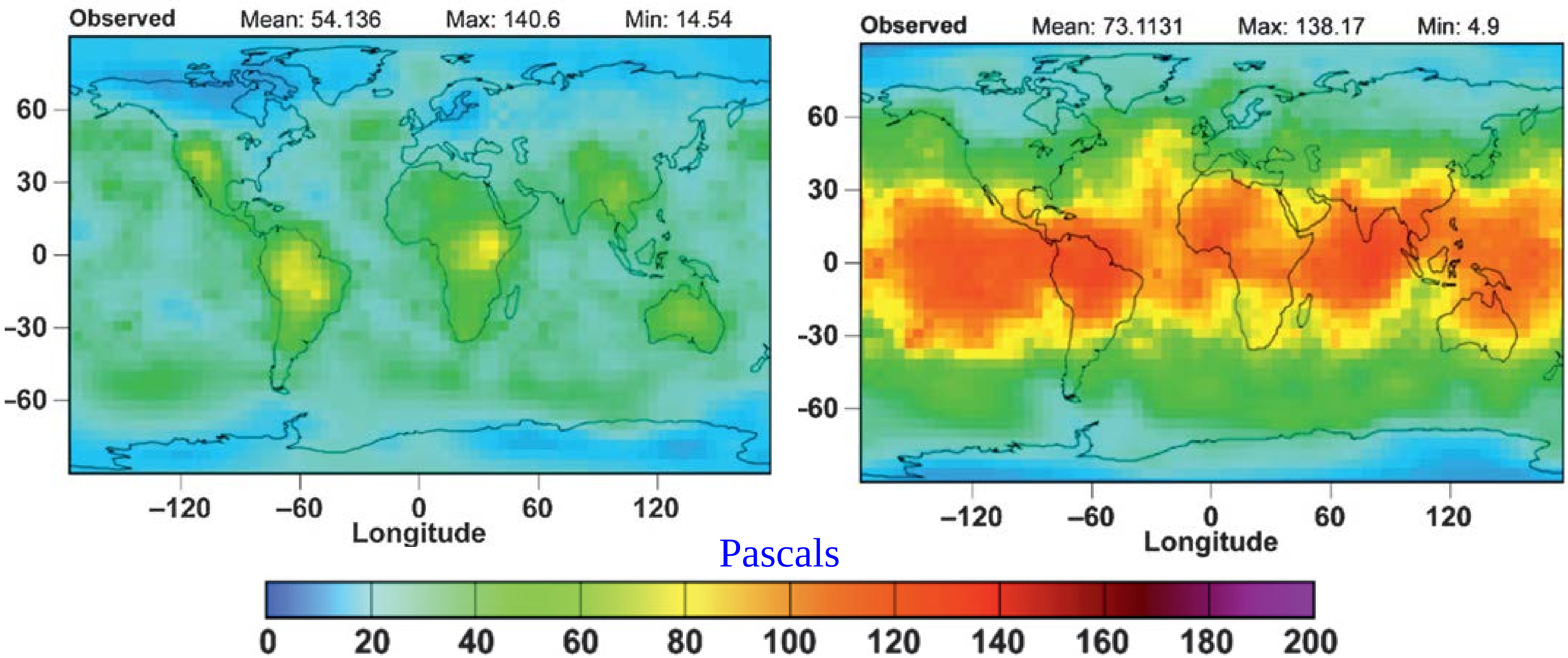

Deep, meridionally broad heating projects very efficiently onto the main semidiurnal mode.
O_3 contributes to zonally uniform response

Diurnal tide is weaker, more localized to continental regions .

Covey et al., *JAS 68*, 2011

Diurnal and Semidiurnal Tide

Normalized amplitude (%)

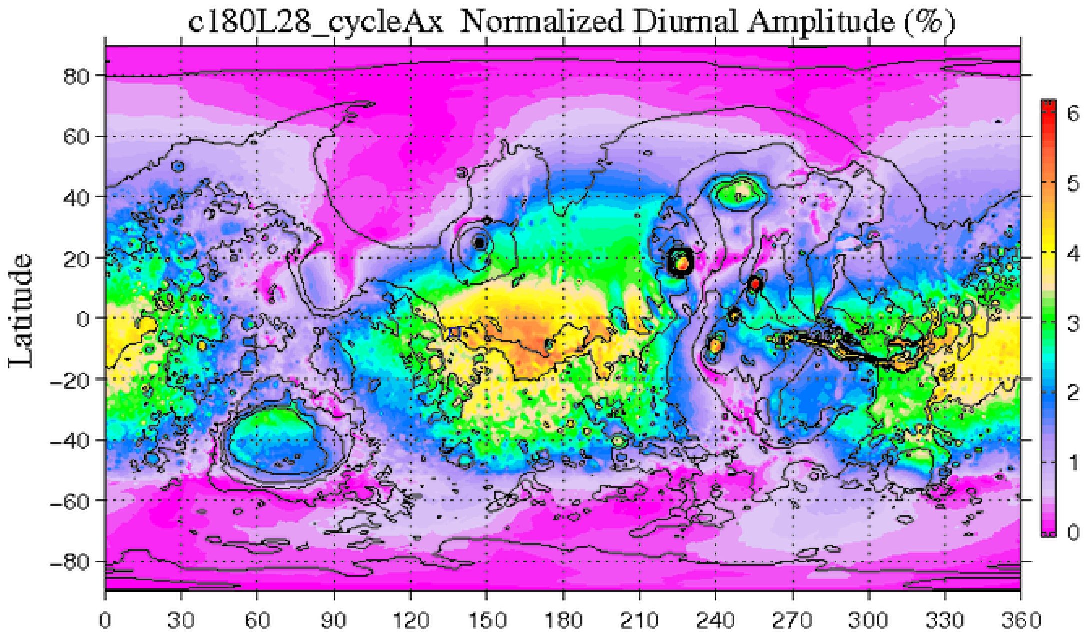

Longitude

$L_s = 160°$

c180: 0.5°x0.5°

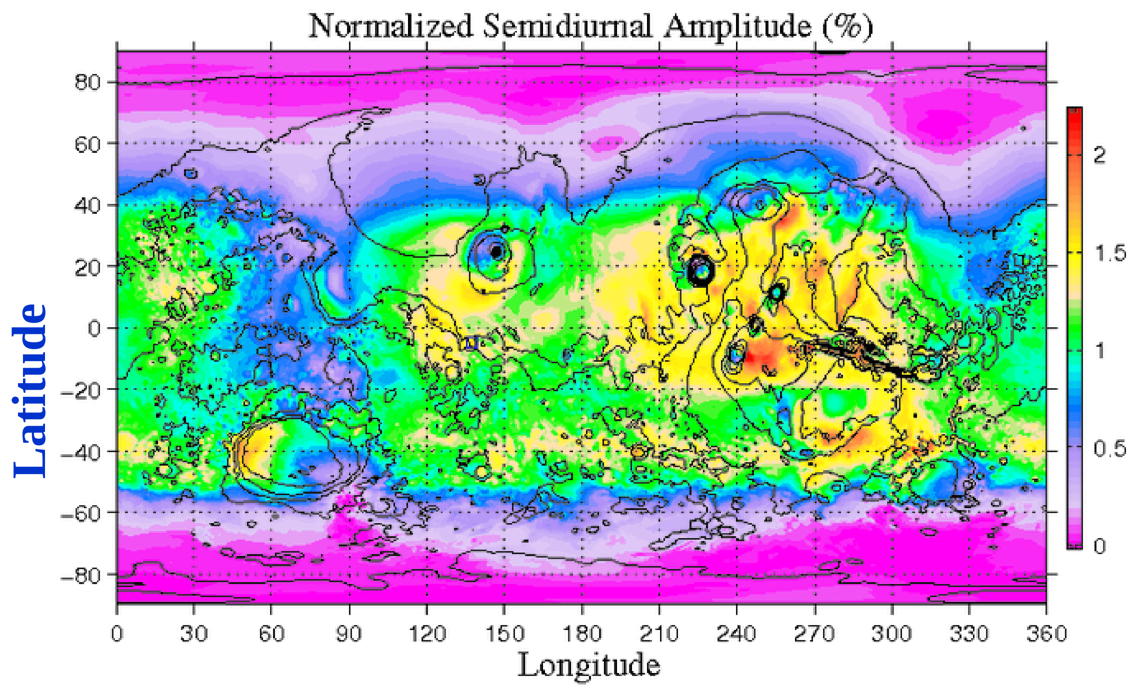

Diurnal and Semidiurnal Surface Pressure Oscillations at VL1 (22^o N)

4 Year record at Viking Lander 1

Amp= P_{tide}/P_{diavg}

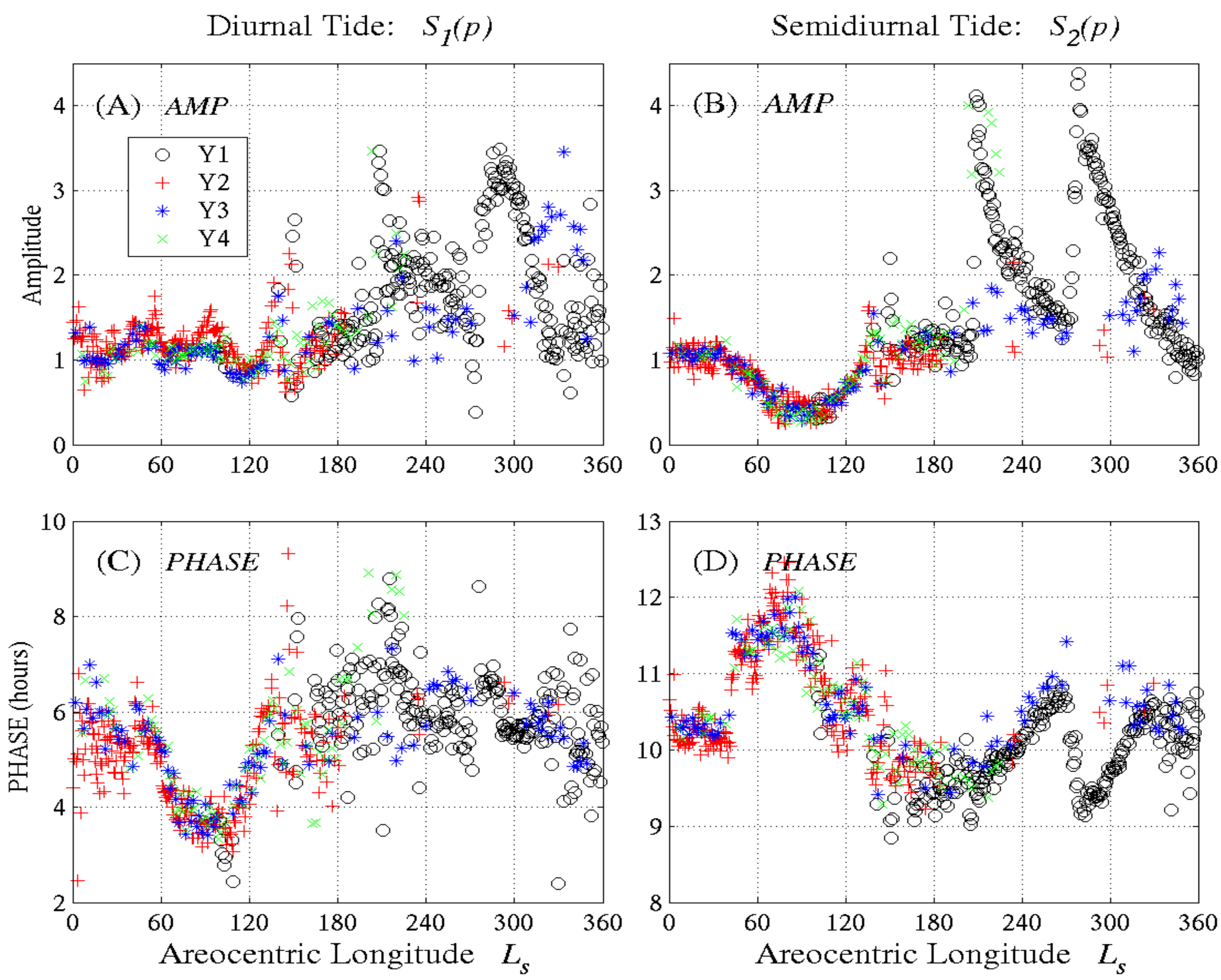

High degree of regularity in the L_s=0-180 period

Viking Surface Pressure Data

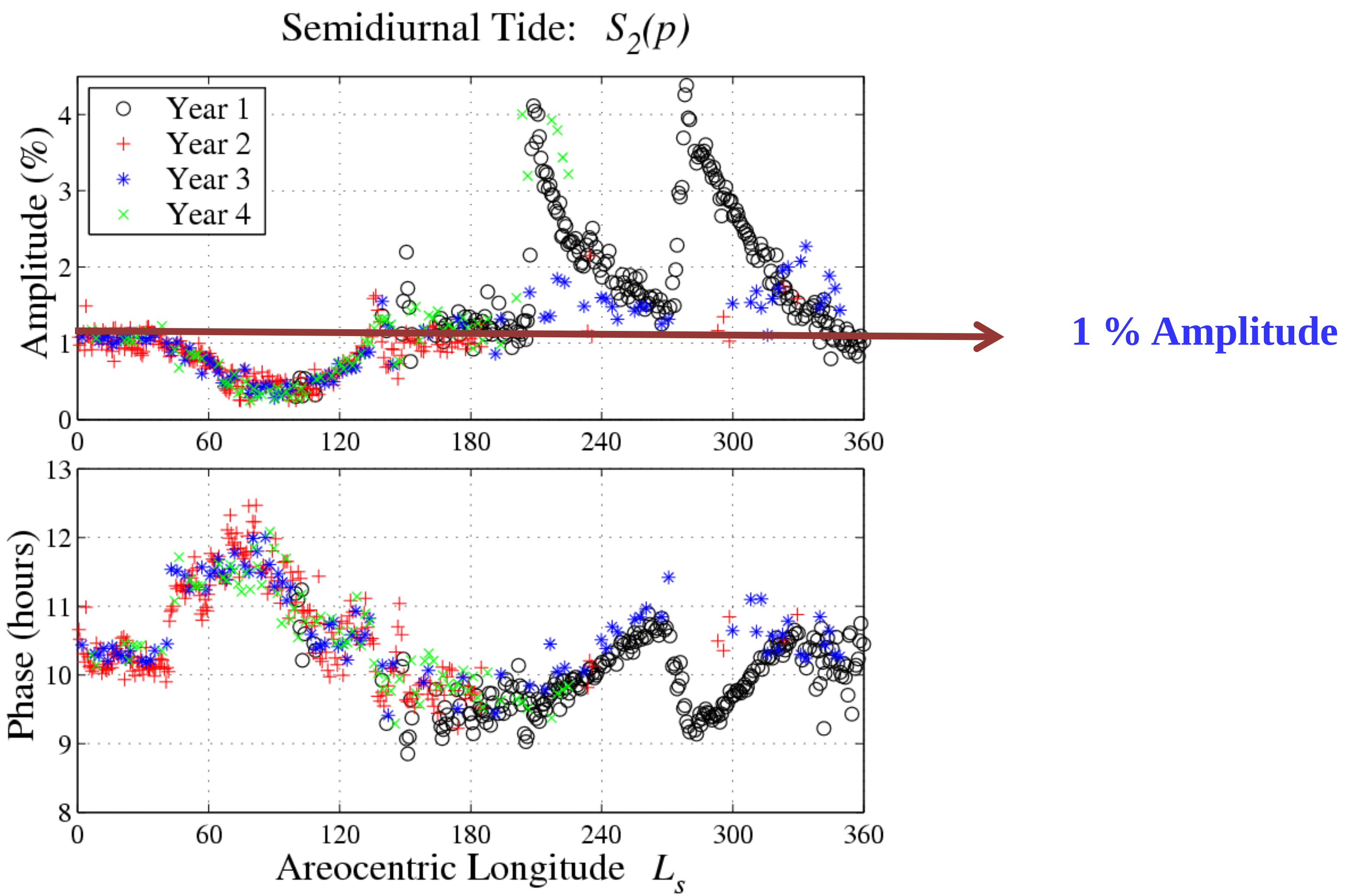

Consistent Tide response over 4 Mars years: MY12-15

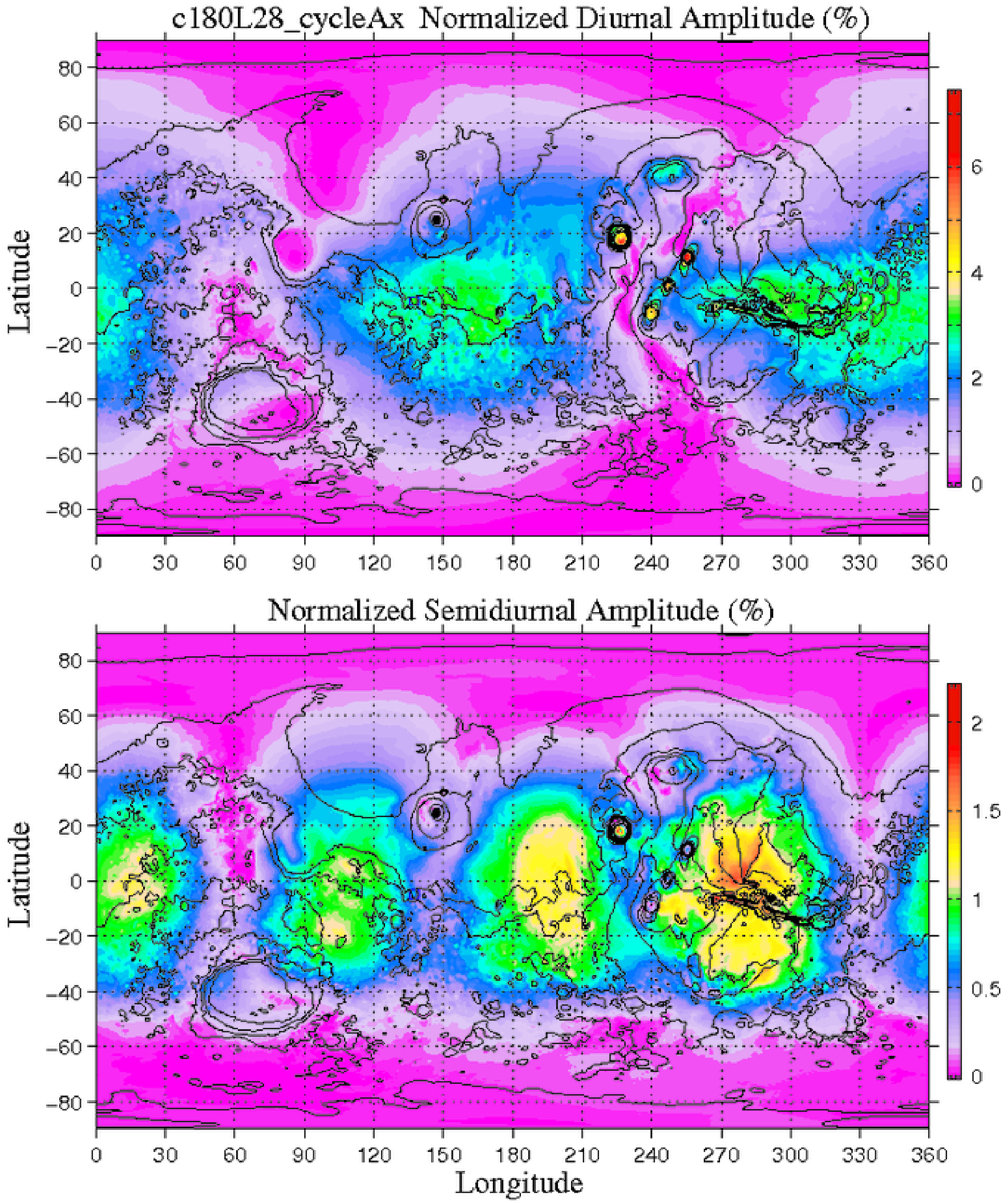
c180L28_cycleAx Normalized Diurnal Amplitude (%)
Latitude
80
60
40
20
0
−20
−40
−60
−80
0
30
60
90
120
150
180
210
240
270
300
330
360
6
4
2
0
Normalized Semidiurnal Amplitude (%)
Latitude
Longitude
2
1.5
1
0.5
0

Ls= 100

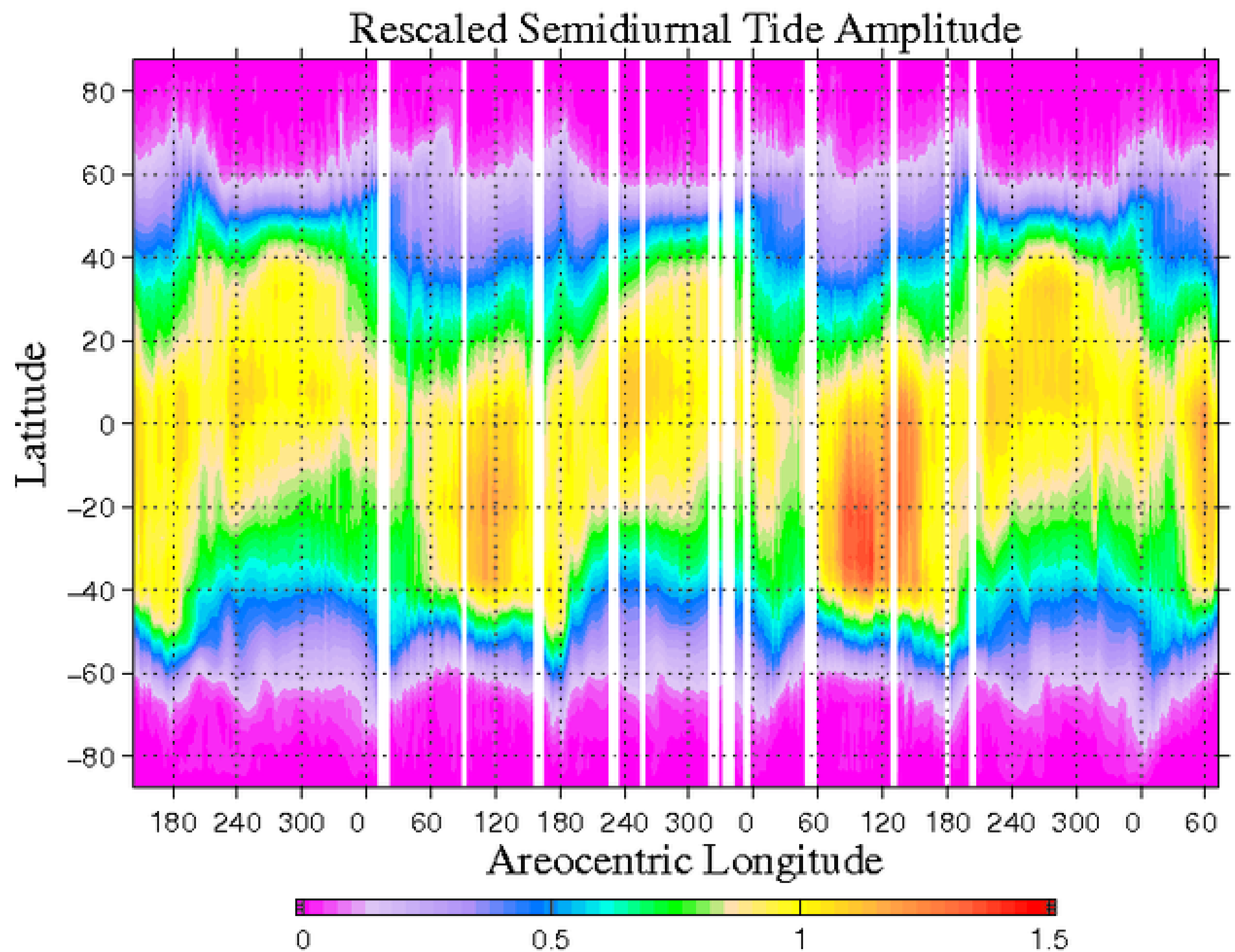

Rescaled Semidiurnal Tide Amplitude
Latitude
80
60
40
20
0
-20
-40
-60
-80
180 240 300 0 60 120 180 240 300 0 60 120 180 240 300 0 60
Areocentric Longitude
0
0.5
1
1.5

Simulated Surface Pressure Amplitude and Phase : L_s~90°

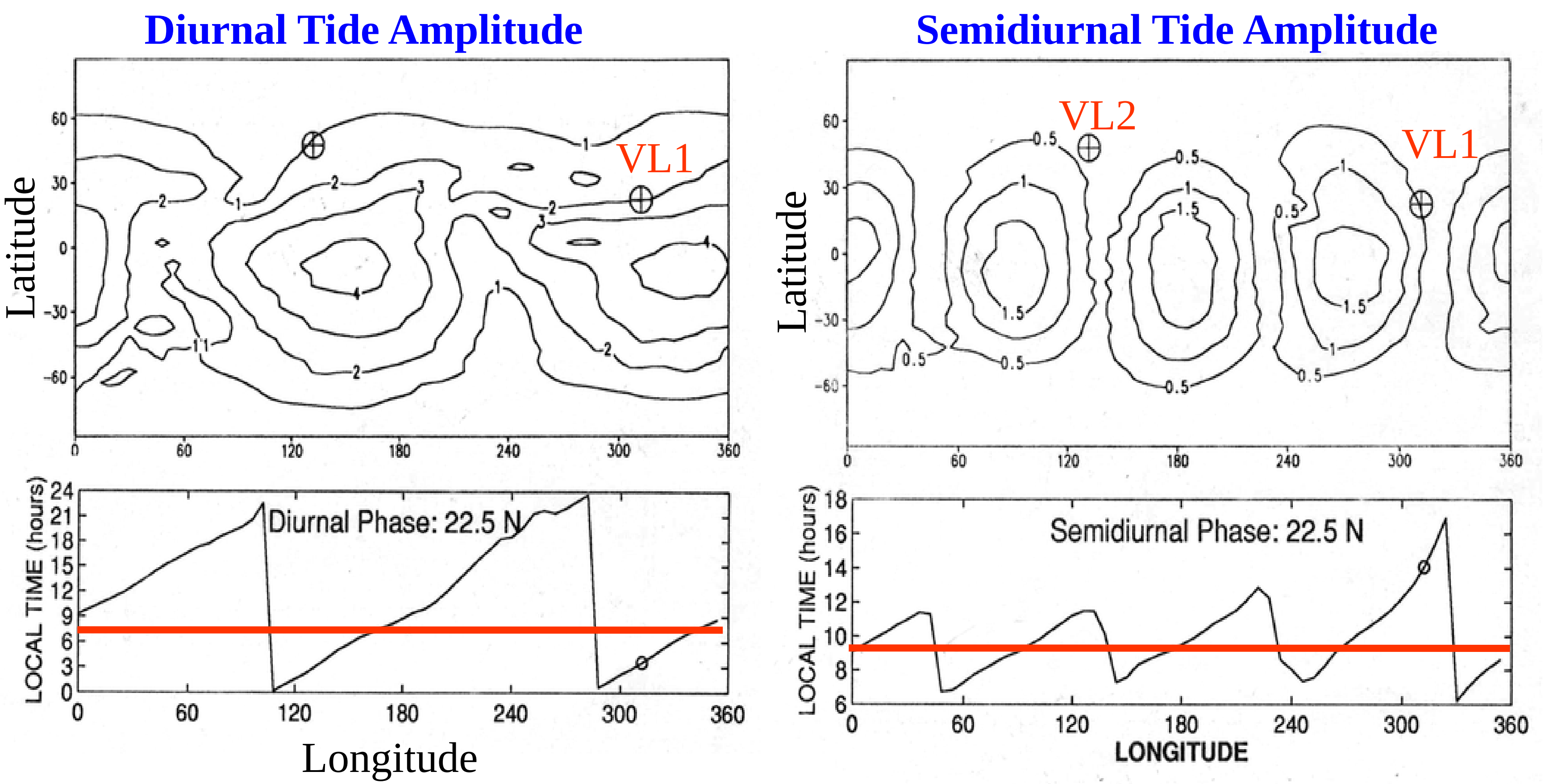

Simulated Surface Pressure Amplitude and Phase : $L_s \sim 90^{o}$

Diurnal Tide Amplitude

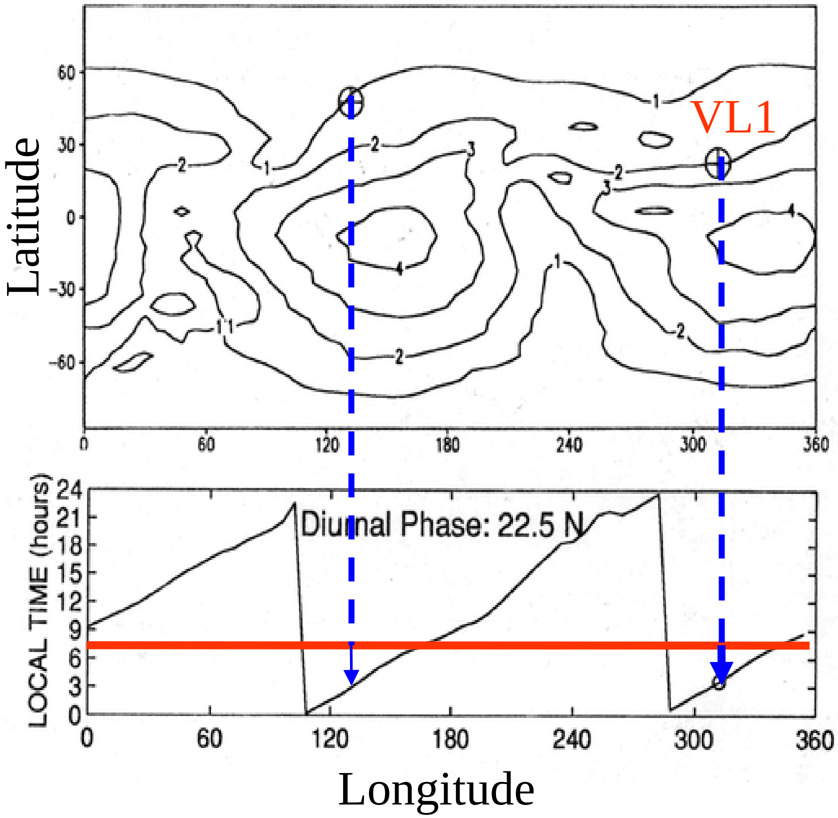

Semidiurnal Tide Amplitude

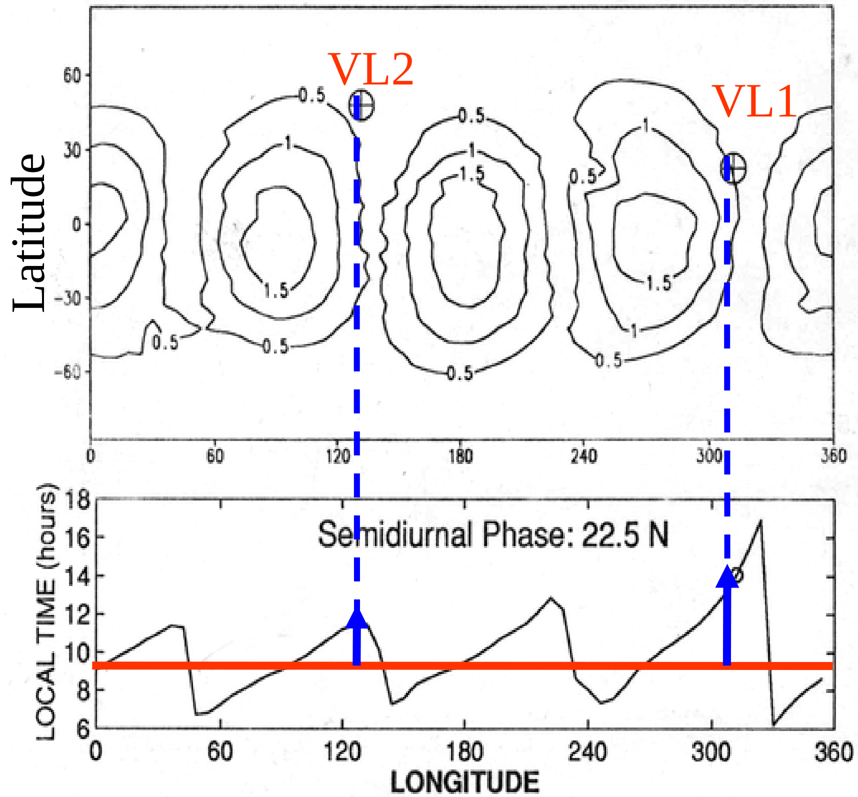

Wave 2 Interference Pattern

- S_1 & DK1 modes dominant
- Simultaneous Phase Advance at two lander sites for diurnal tide as DK1 increases –As observed

Wave 4 Interference Pattern

- S_2 & SDK2 modes dominant
- Simultaneous Phase Delay for Semidiurnal tide as SDK2 increases As observed

Semidiurnal Tide (22°N): Envelope of Seasonal Variation

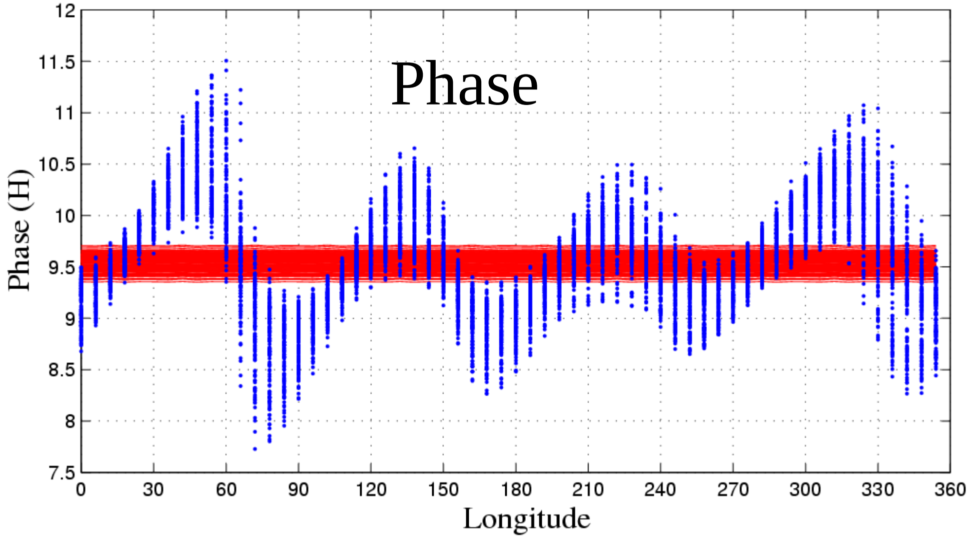

Amplitude

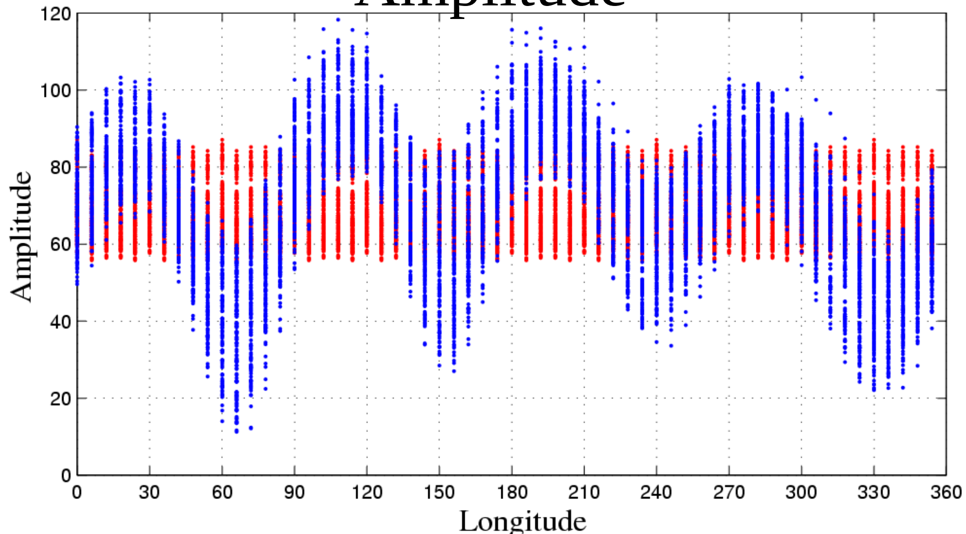

Longitude

Fixed Dust simulation:

Local Tide

Migrating component

Migrating tide phase is relatively invariant

Relatively little variation in migrating tide amplitude over season (~40%)---much larger longitudinal variation.

Westward migrating solar radiation modulated by topographic influences

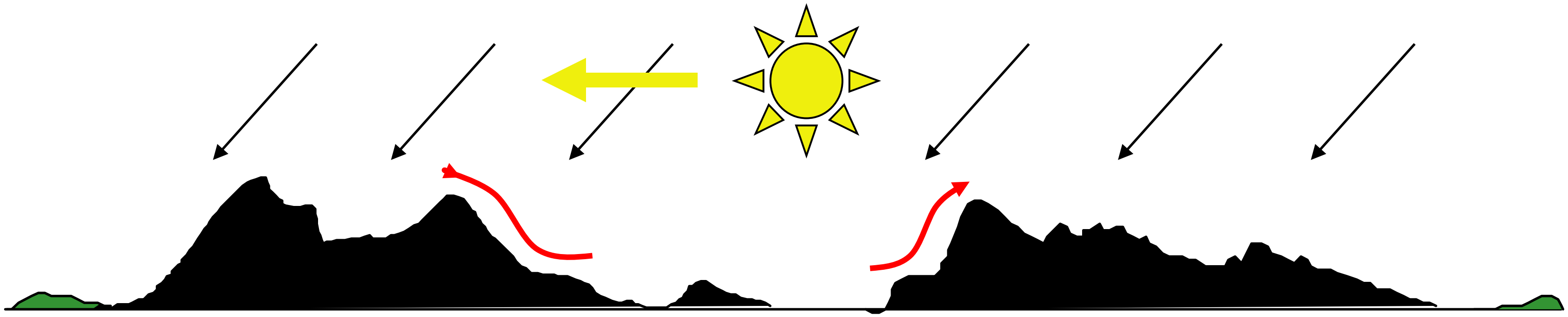

$\cos(\Omega t + \lambda)$ $\cos 2\lambda$ ⟶ $\cos(\Omega t + 3\lambda) + \cos(\Omega t - \lambda)$

solar radiation — **topography m = 2** — **diurnal, westward s=3** — **diurnal eastward s=1 DK1**

Similarly, $\cos(2\Omega t + 2\lambda)\cos 4\lambda$ yields $\cos(2\Omega t - 2\lambda)$ **SDK2**

Similarly, $\cos(\Omega t + \lambda)\cos 3\lambda$ yields $\cos(\Omega t - 2\lambda)$ **DK2**

Migrating tides are scattered into nonmigrating tides; induced upslope/downslope winds play a significant role

Simulated Semidiurnal Tide at VL1: Amplitude and Phase

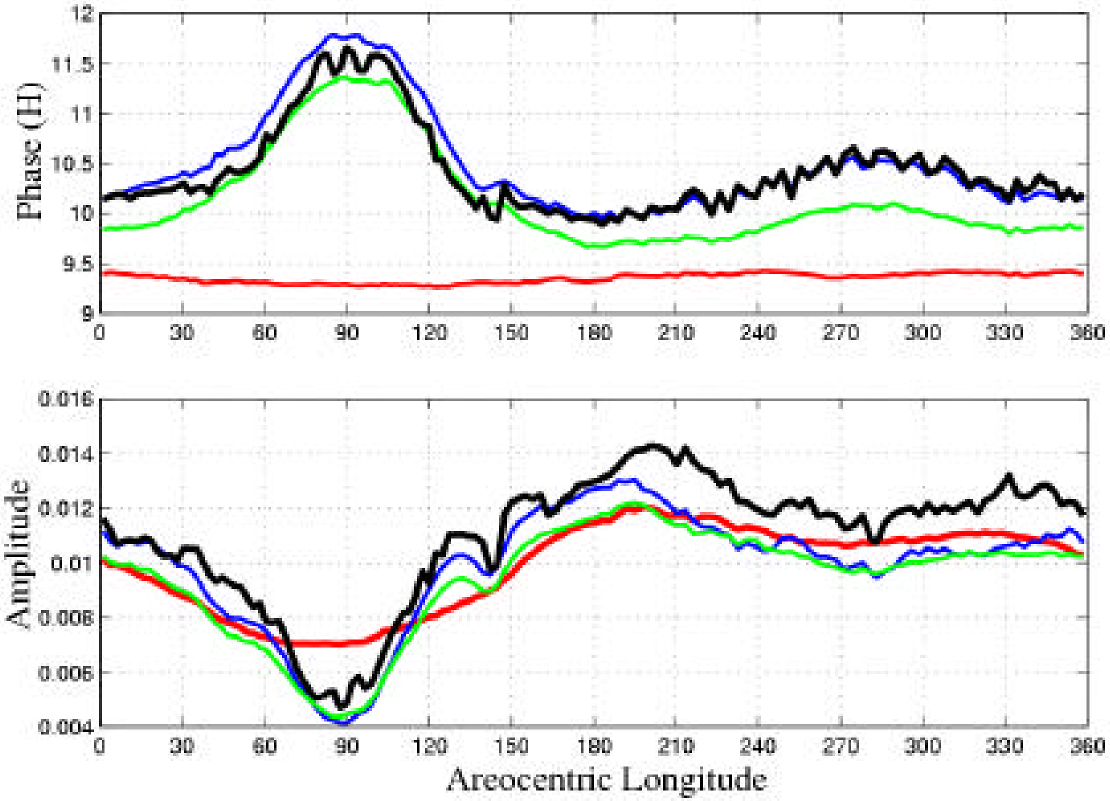

Fixed dust simulation

--- Simulated SD at VL1

--- S2 mode only

--- S2 + SDK2

Diurnal Kelvin Wave in MACDA Psfc

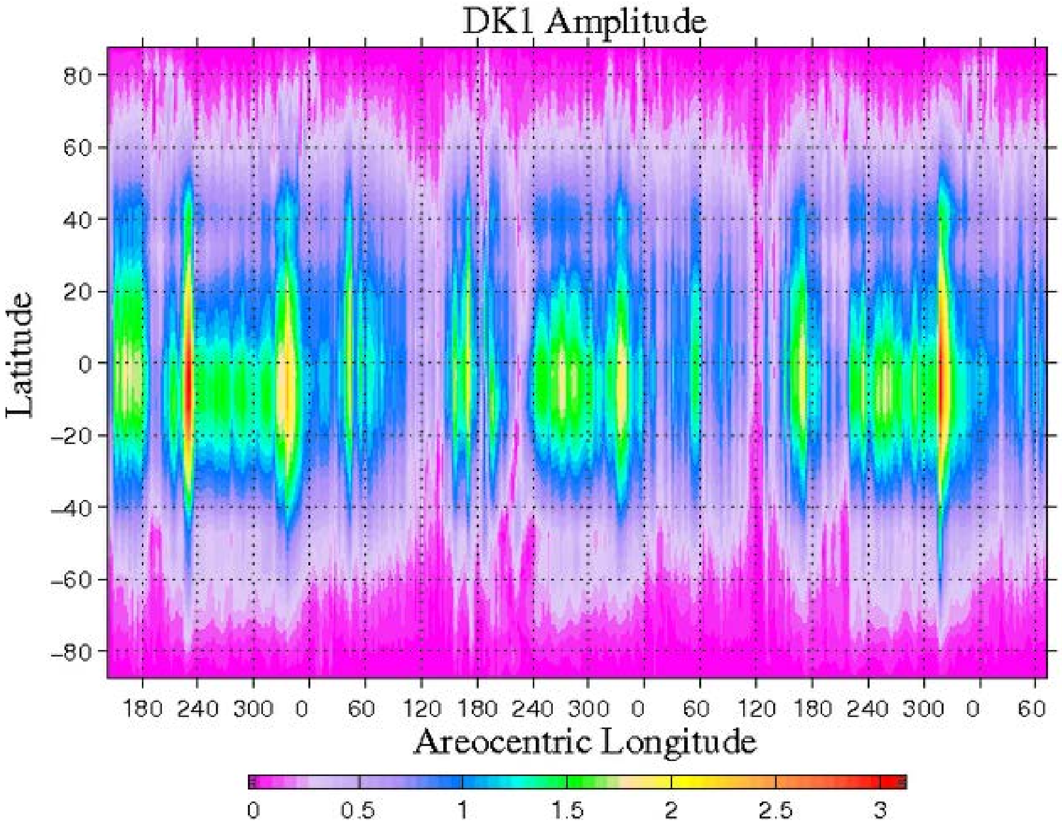

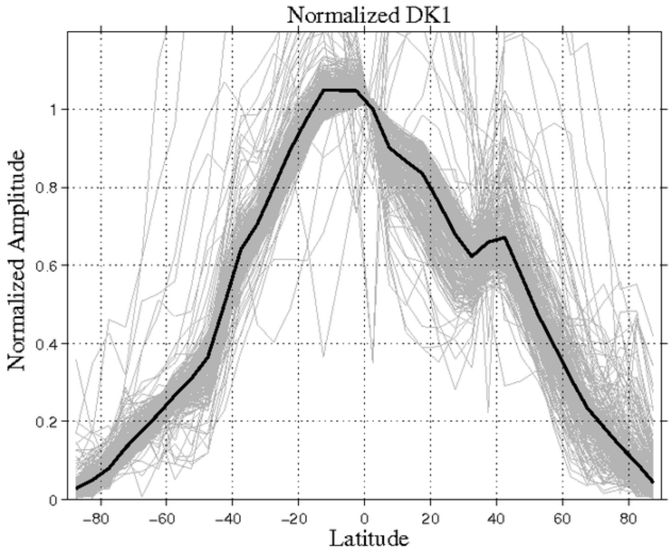

DK1 Amplitude

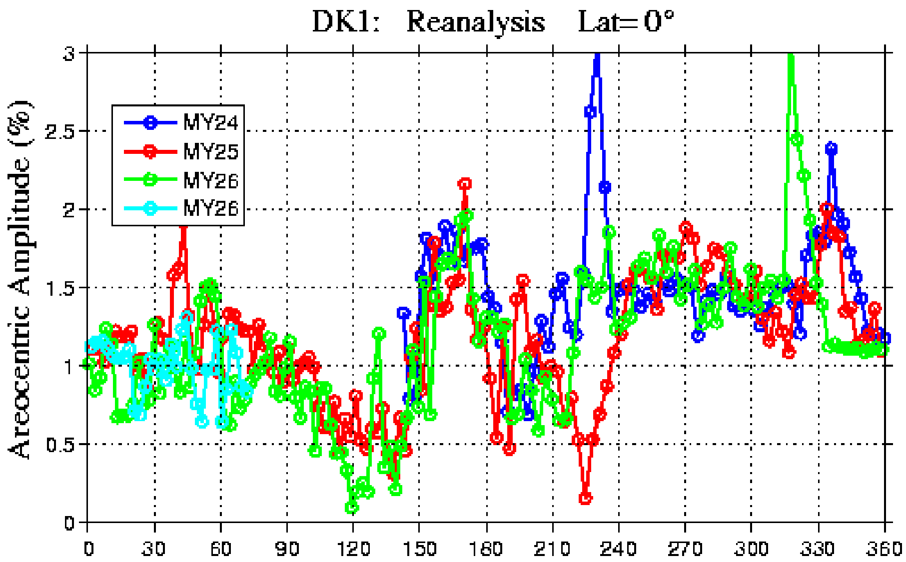

Reanalysis

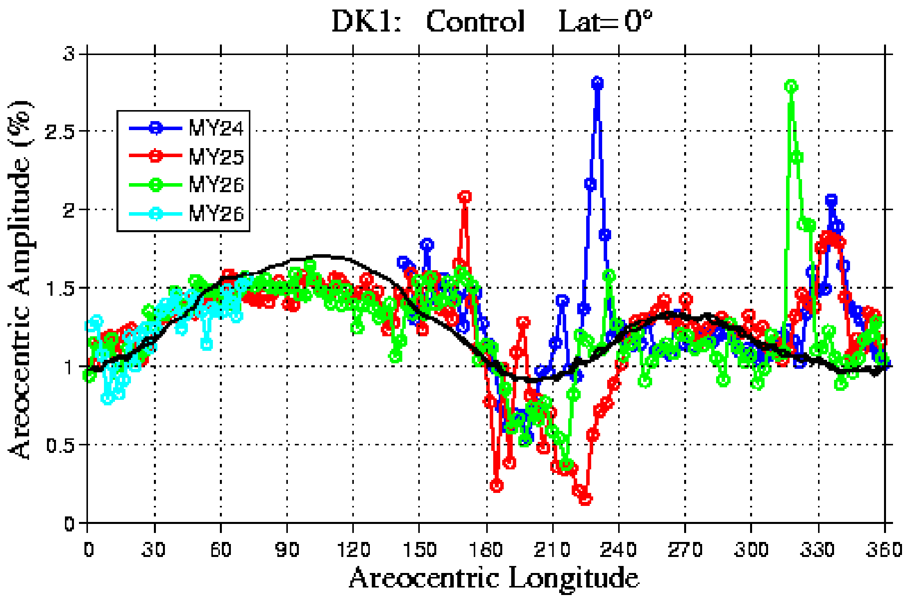

Control Run
and Fixed Dust run (black)

DK1 Amplitude

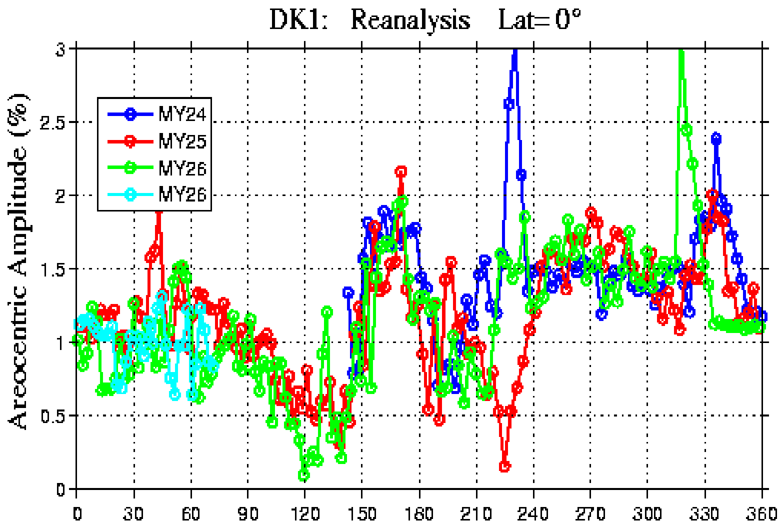

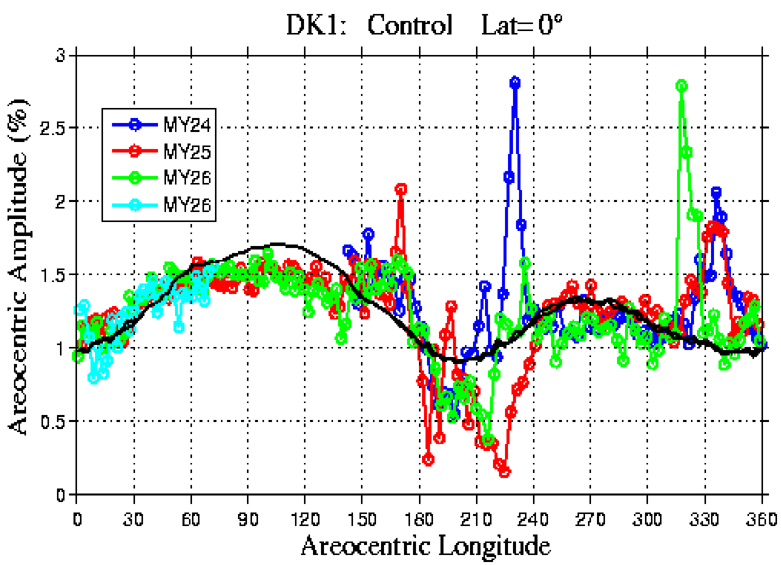

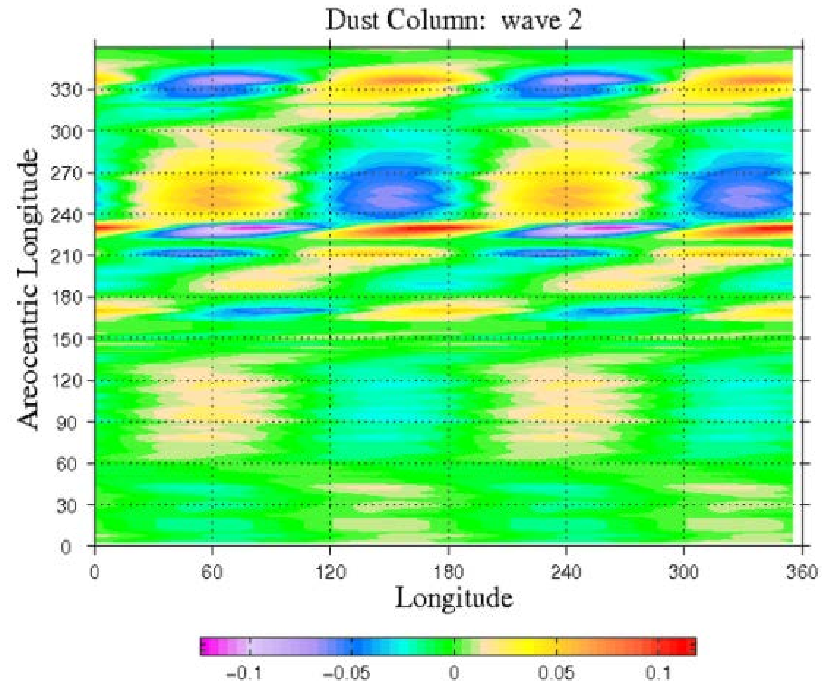

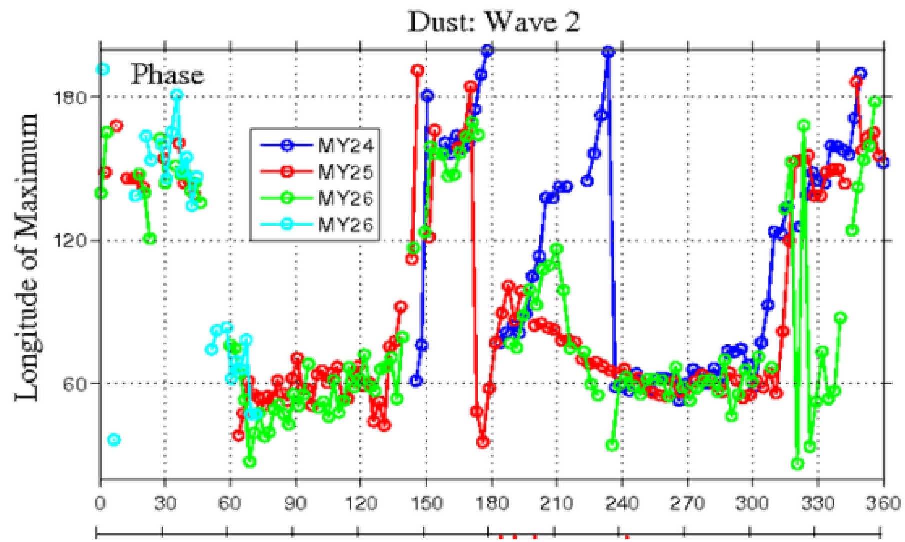

Equatorial Nighttime Clouds and Temperatures

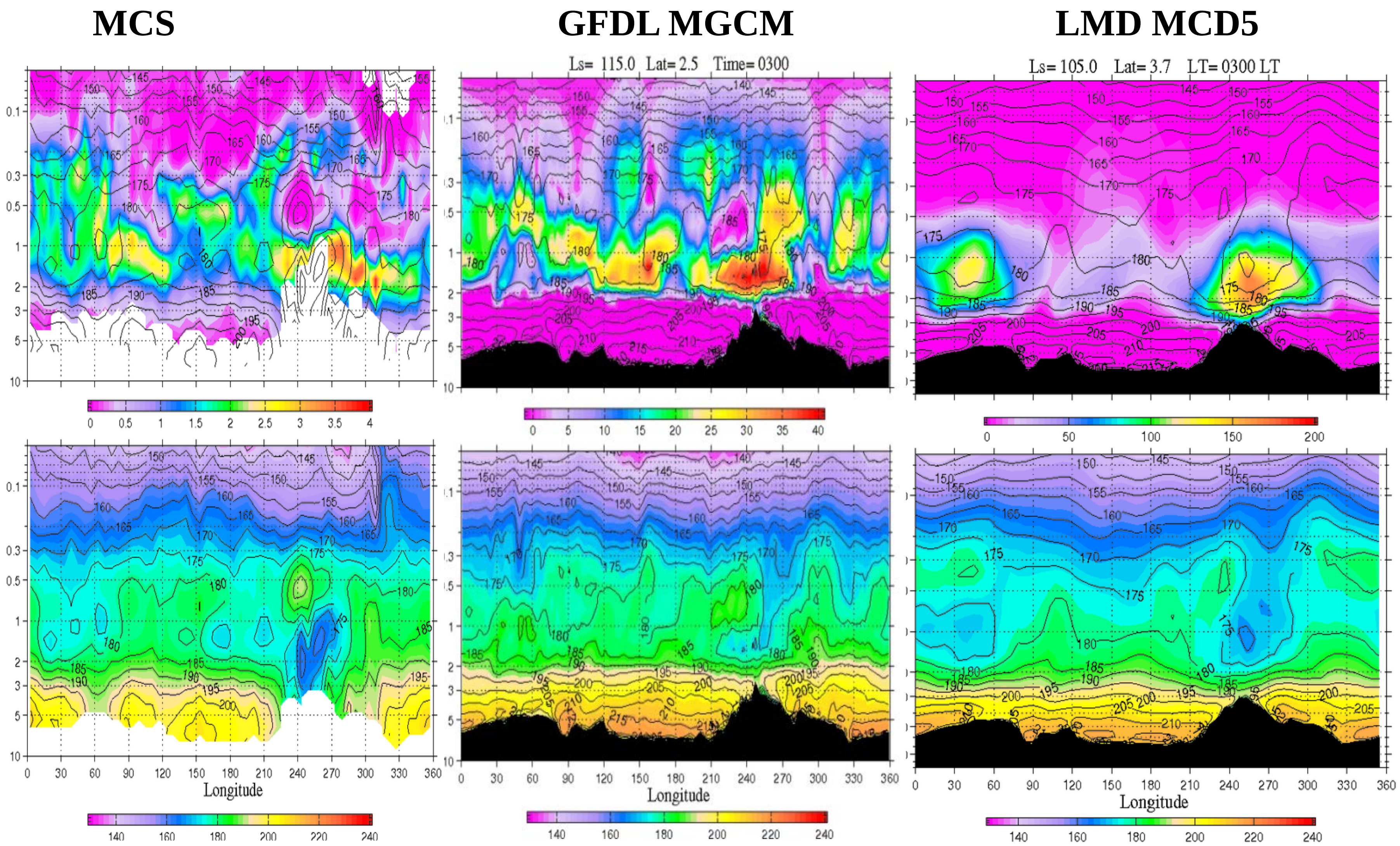

0300 LT Clouds and Temperature MCS

L_s= 110-120°

Lat = -2.5-2.5° Lon= 250-260° E

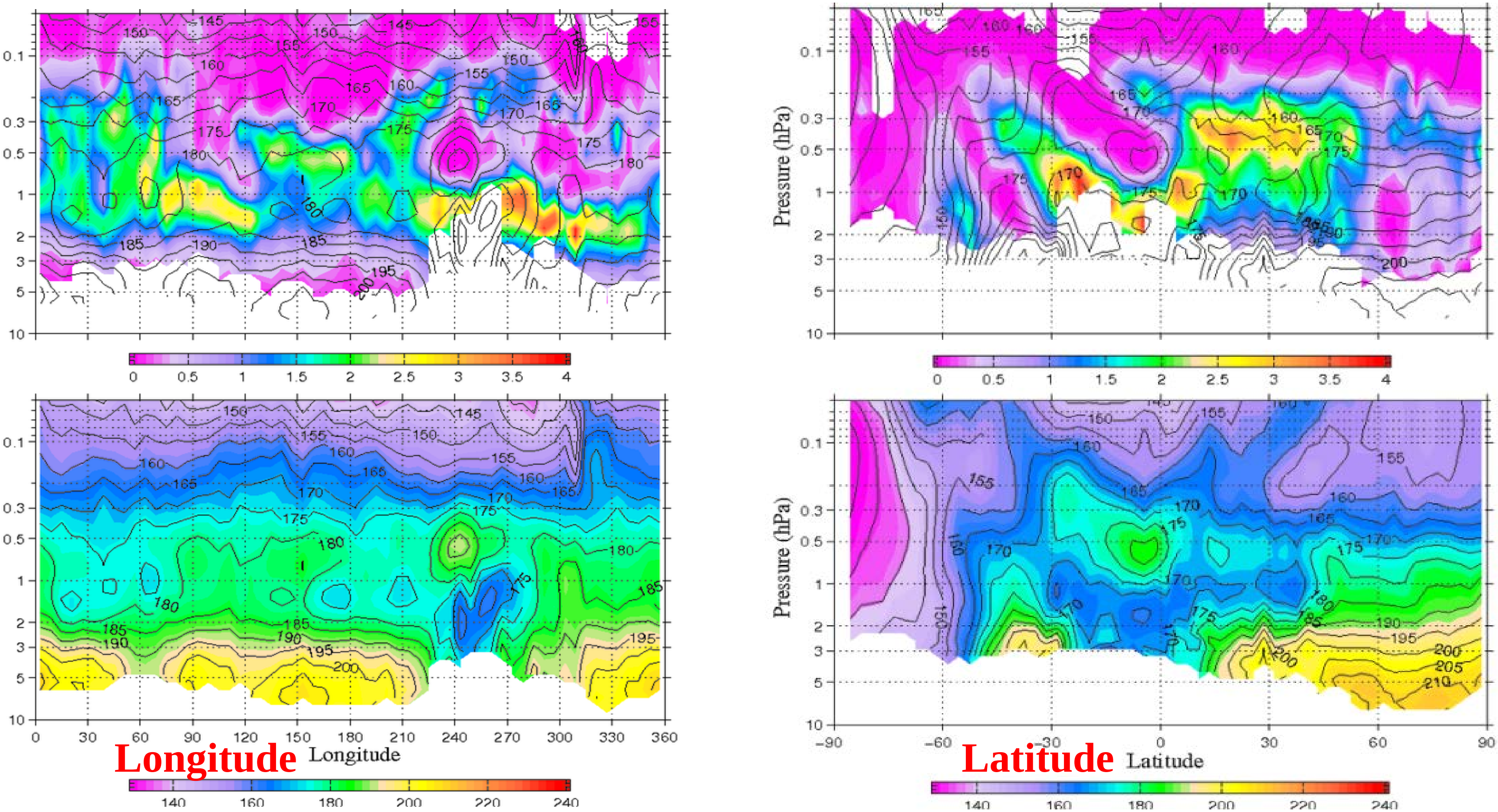

Figure 30. Longitude/pressure sections of equatorial cloud opacity (top row) and temperature (bottom row). Temperature contoured in intervals of 5 K in all plots. Cloud opacity Δτ is shaded in units of $10^{-3}\ km^{-1}$

Diurnal Variation of Cloud and Temperature

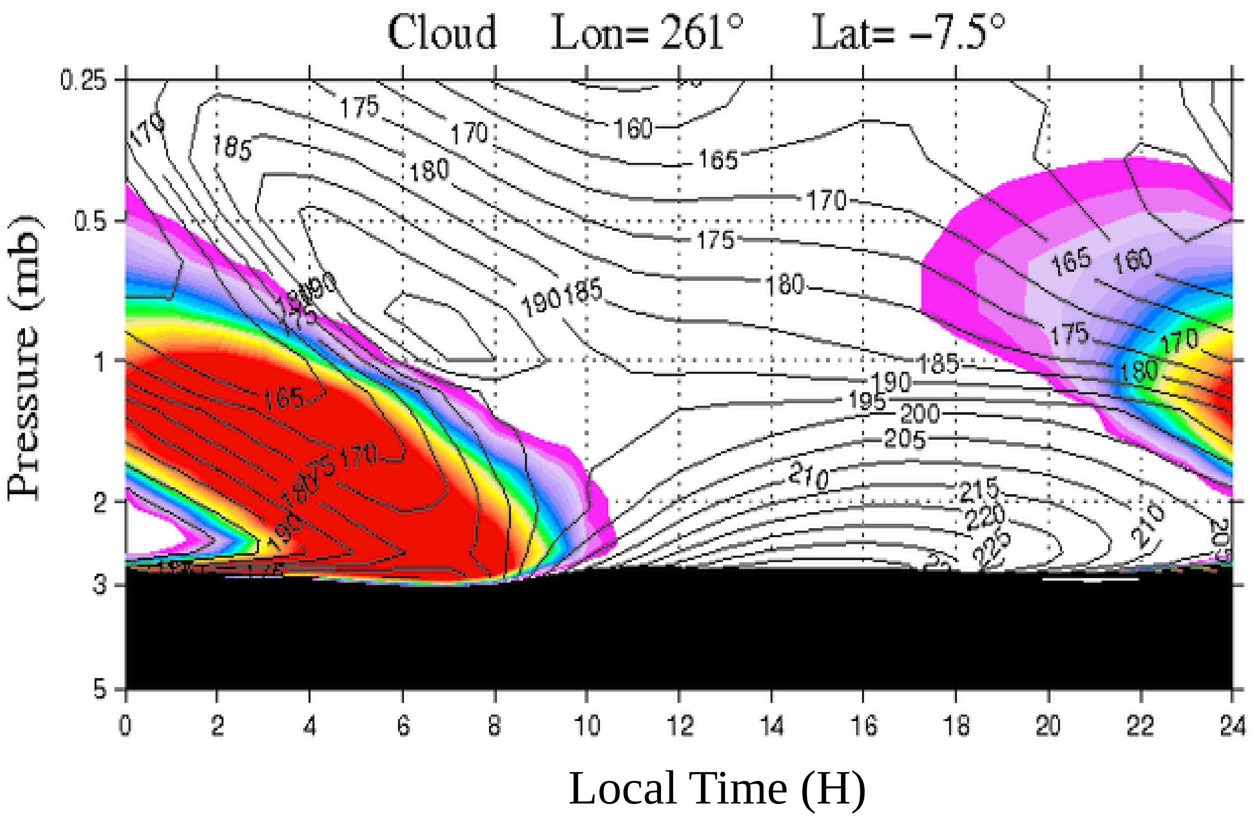

Mars Climate Sounder MCS

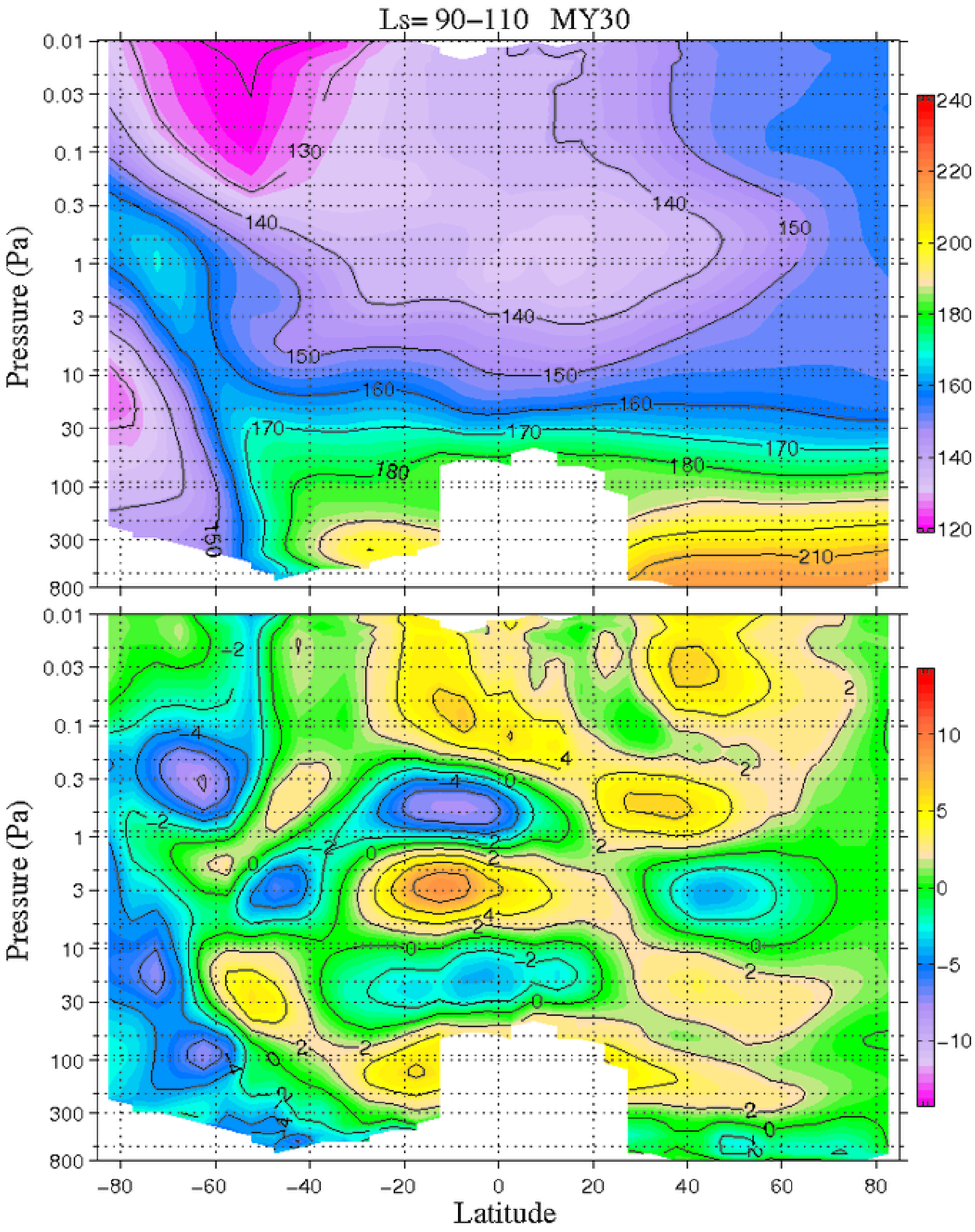

Zonally-averaged Temperature
0-80 km

$T_{avg} = (T_{3pm} + T_{3am})/2$

Diurnal Average*

$T_{diff} = (T_{3pm} - T_{3am})/2$

Sun-Synchronous Tide*

aka Migrating Tide

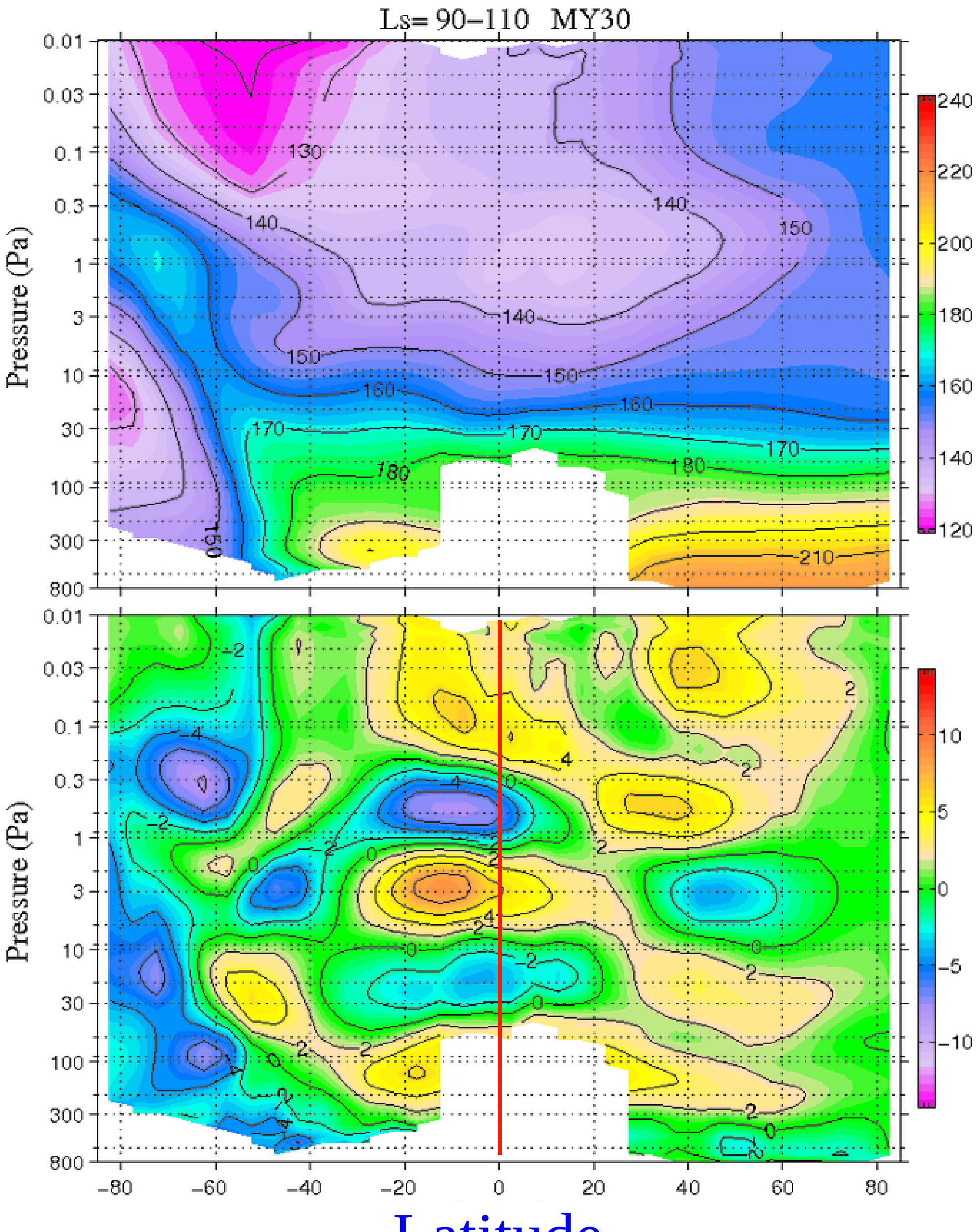

Zonal variations in temperature:

Nonmigrating tide

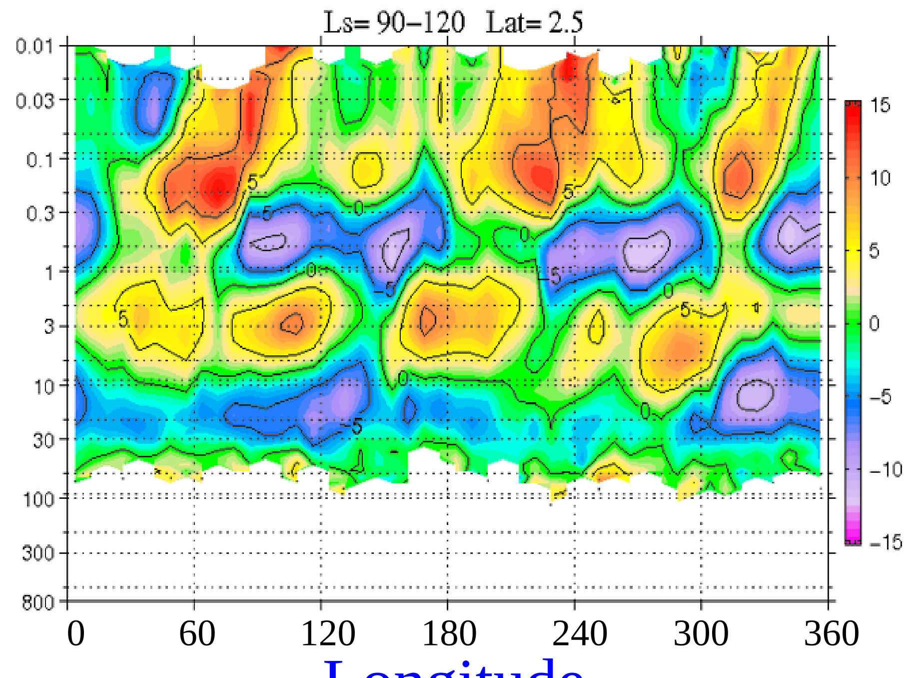

$(T_{3pm} – T_{3am})/2$ @ 2.5N **T'_{3am} @ 2.5N**

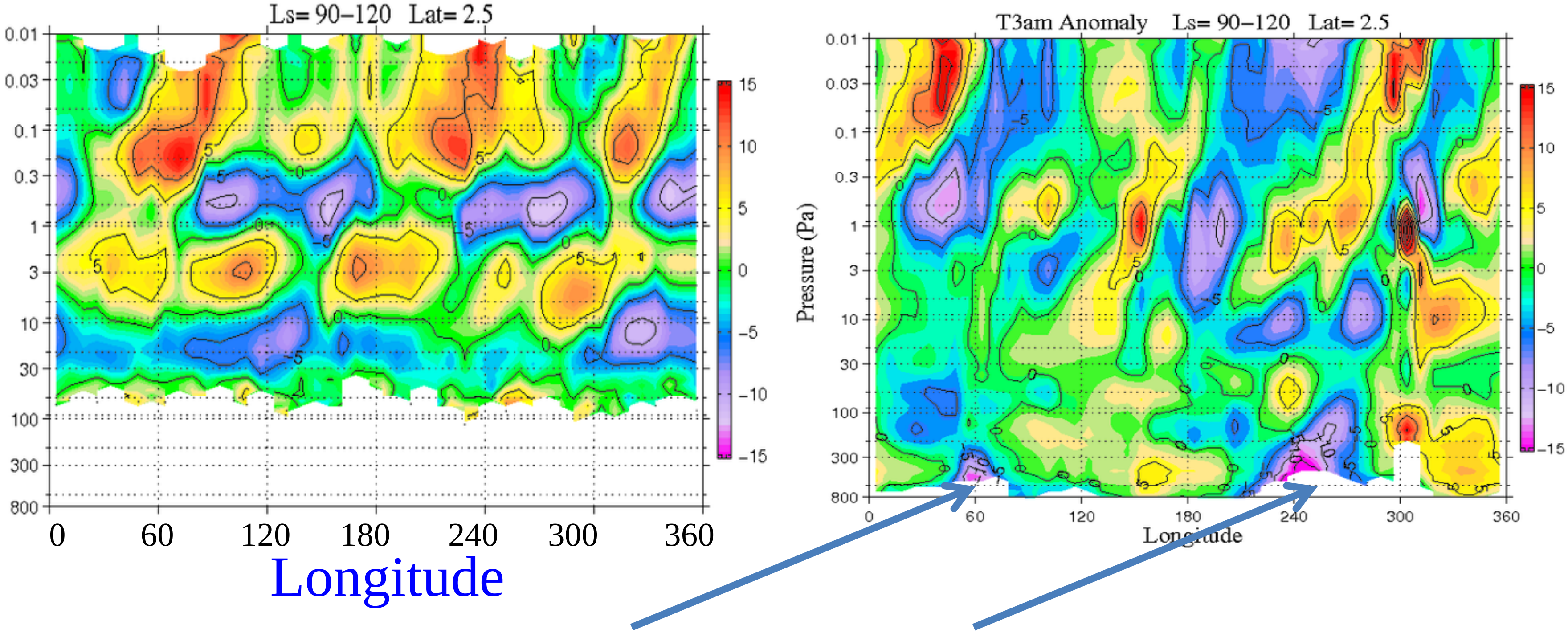

Strong, low-level cooling over Arabia and Tharsis

Nonmigrating Tide Forcing

Topographically Locked Nighttime Water Ice Clouds

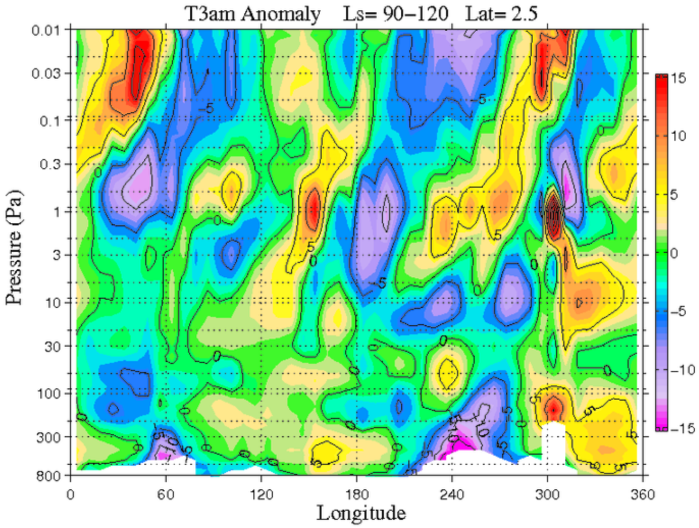

Mars Climate Sounder T_{3am} Anomaly field

and Zonal Wave Components

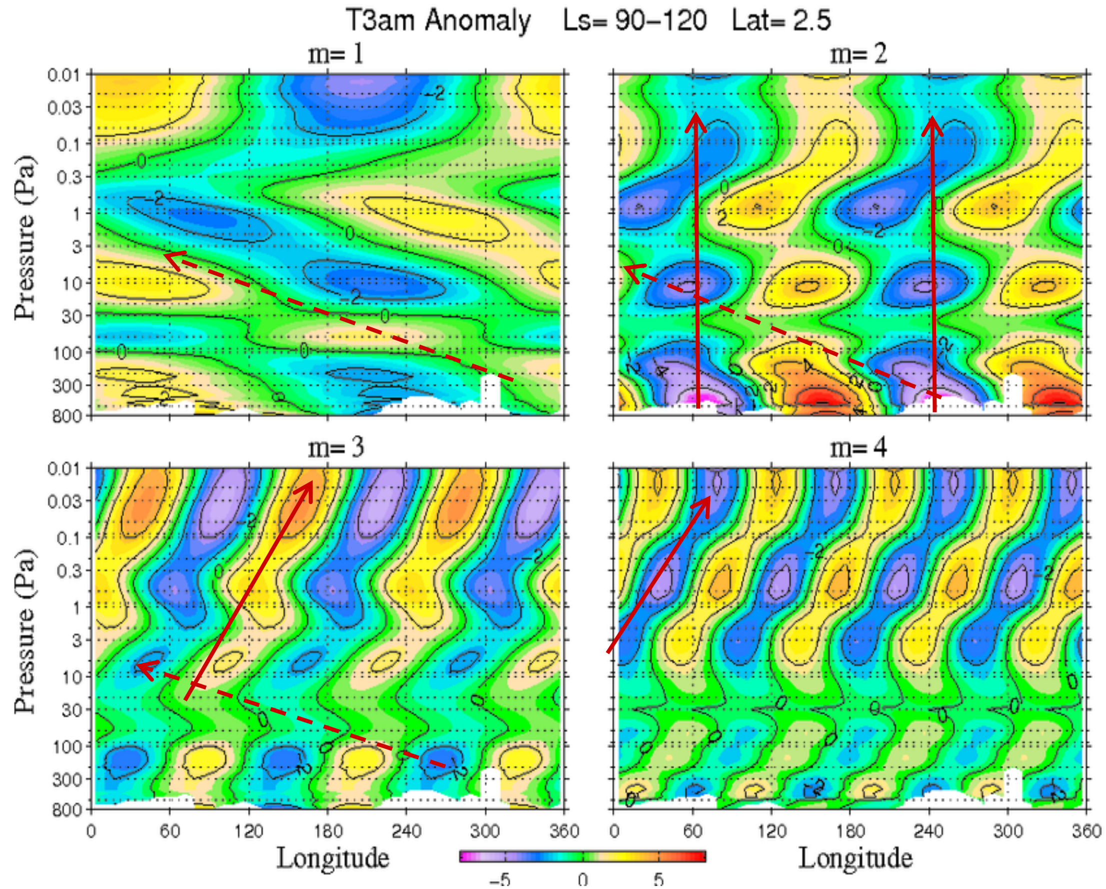

Arrows show pairs of possible wave modes

Prominent DK1 (*m*=2) & DK2 (*m*=3) & DK4(*m*=4)

Kelvin Wave Simulation

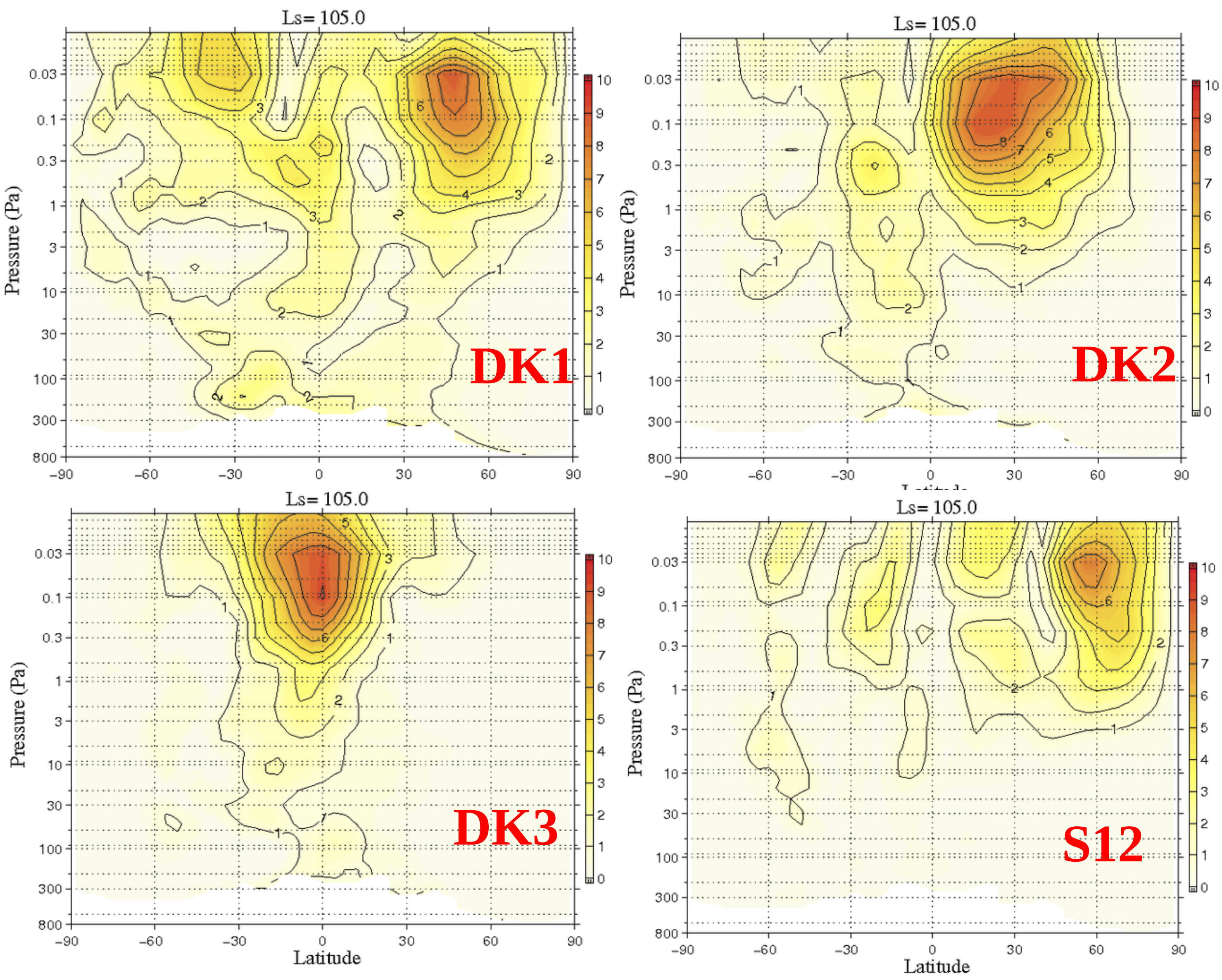

MGCM Simulation of Equatorial Geopotential

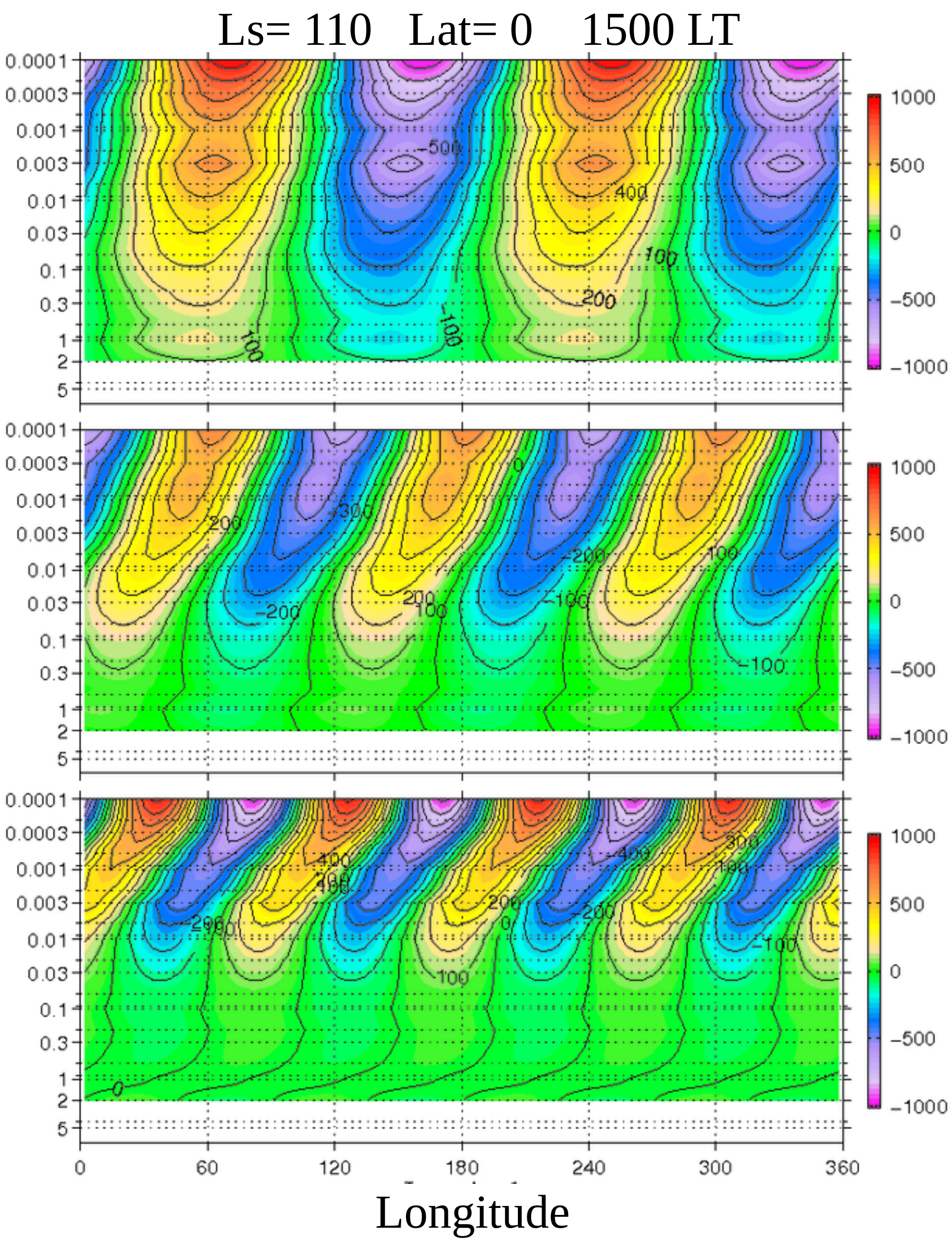

Thermal Tides: Survey of Topics

- Well-defined forcing period: Atmospheric response determined by the horizontal and vertical structure of the forcing: For Mars, sensible and radiative exchange with the surface and absorption of insolation by airborne dust are dominant forcing mechanisms.
- Well-developed Linear Tide Theory provides a basis for relating temperature structure and forcing.
- Examples of diurnal variability in the Martian atmosphere
- Temperature Structure
- Diurnal variation in boundary layer winds: dependence on slope and dust
- Surface pressure variation, focusing on the dependence of the migrating semidiurnal tide on aerosol opacity .

Solar Forcing ---- Diurnal and Semidiurnal harmonics

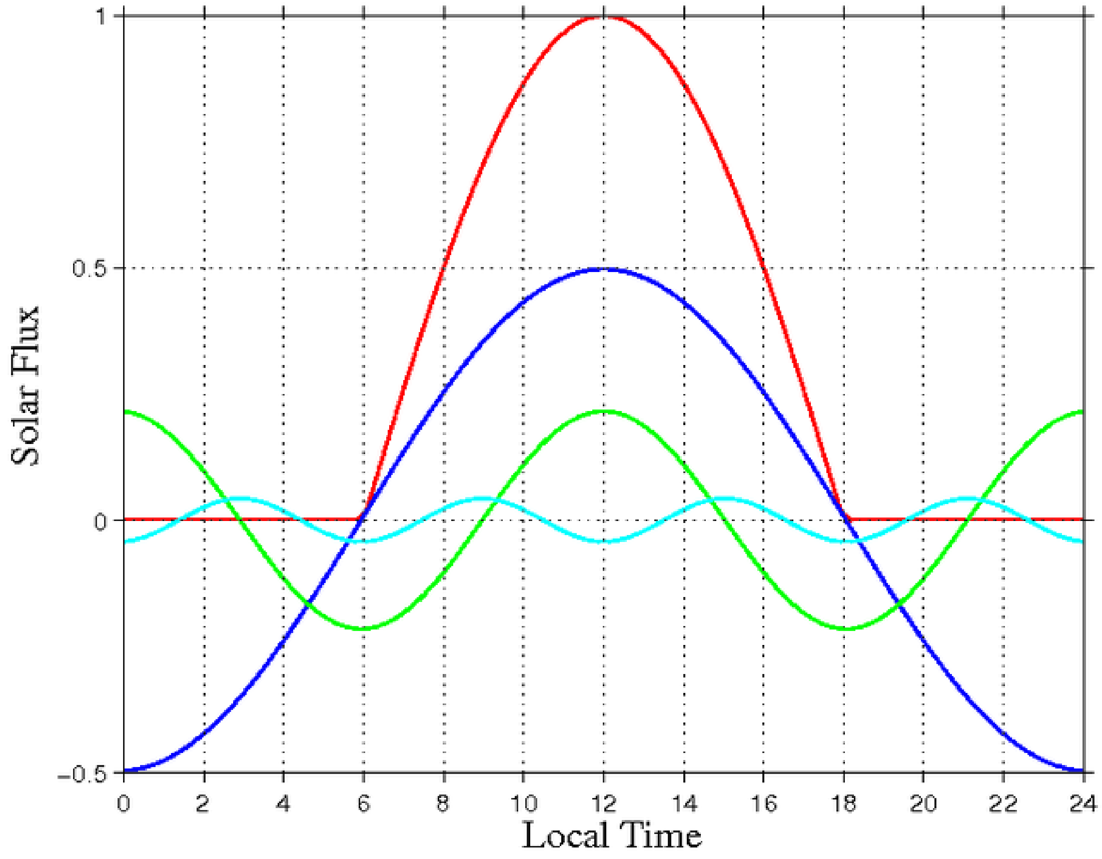

$\sigma = 1, 2, \ldots$

$$F(\lambda, t) \sim \Sigma F_{s,\sigma} \cos[s\lambda + \sigma t]; \quad s = \sigma$$

$$F(\lambda, t_{LT}) \sim \Sigma F_{s,\sigma} \cos[(s-\sigma)\lambda + \sigma t_{LT}] = \Sigma F_{s,\sigma} \cos[\sigma t_{LT}]$$

MCS Tropical Temperature 20S-20N

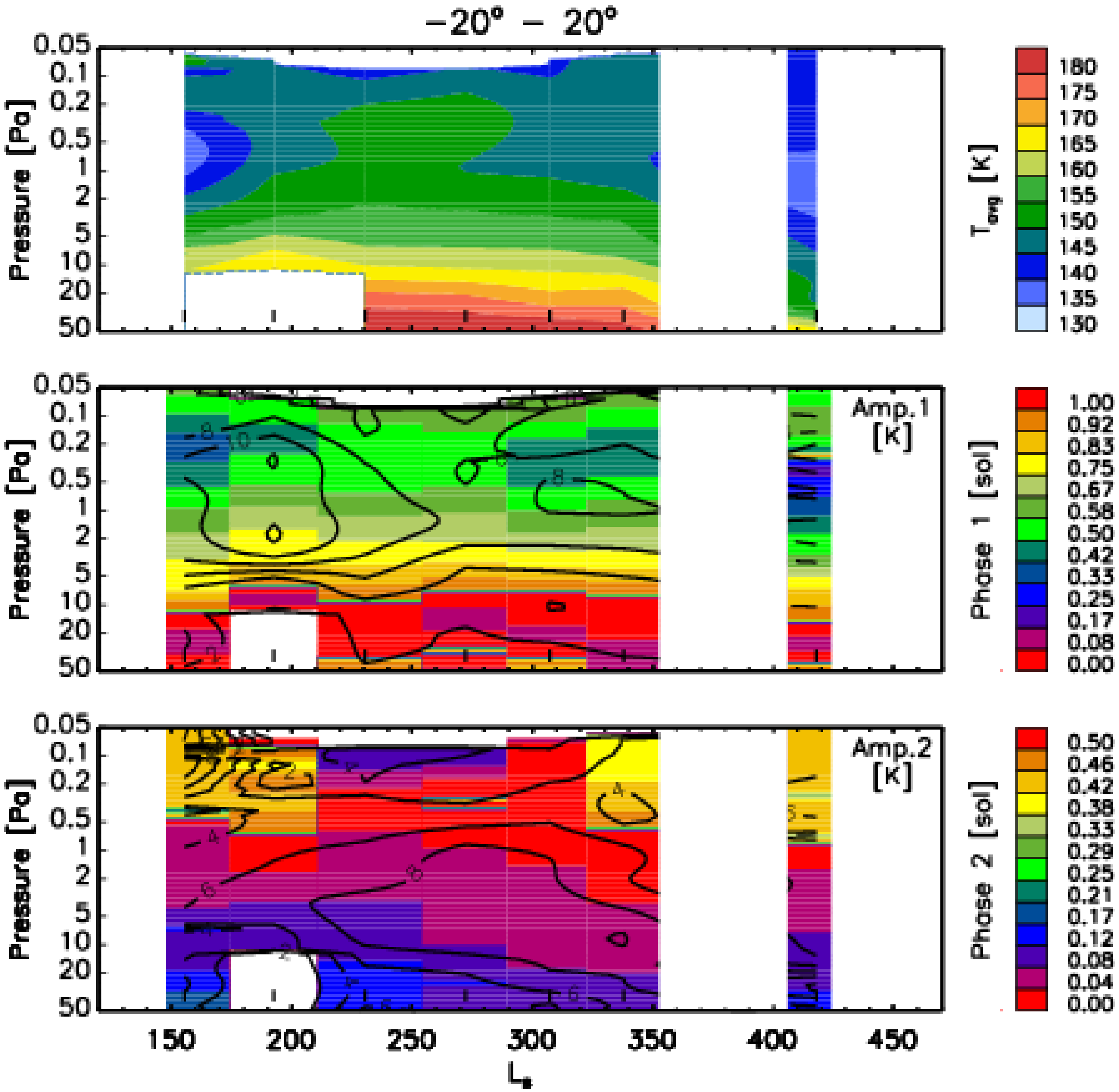

X-track and along-track observations yield up to 6 local times

Allows fitting of diurnal and semidiurnal harmonics of the sun-synchronous tide

Diurnal Tide Amplitude

Semidiurnal Tide Amplitude

Semidiurnal Tide: 5-8 K amplitude in tropics !!

Sun-Synchronous Thermal Tide

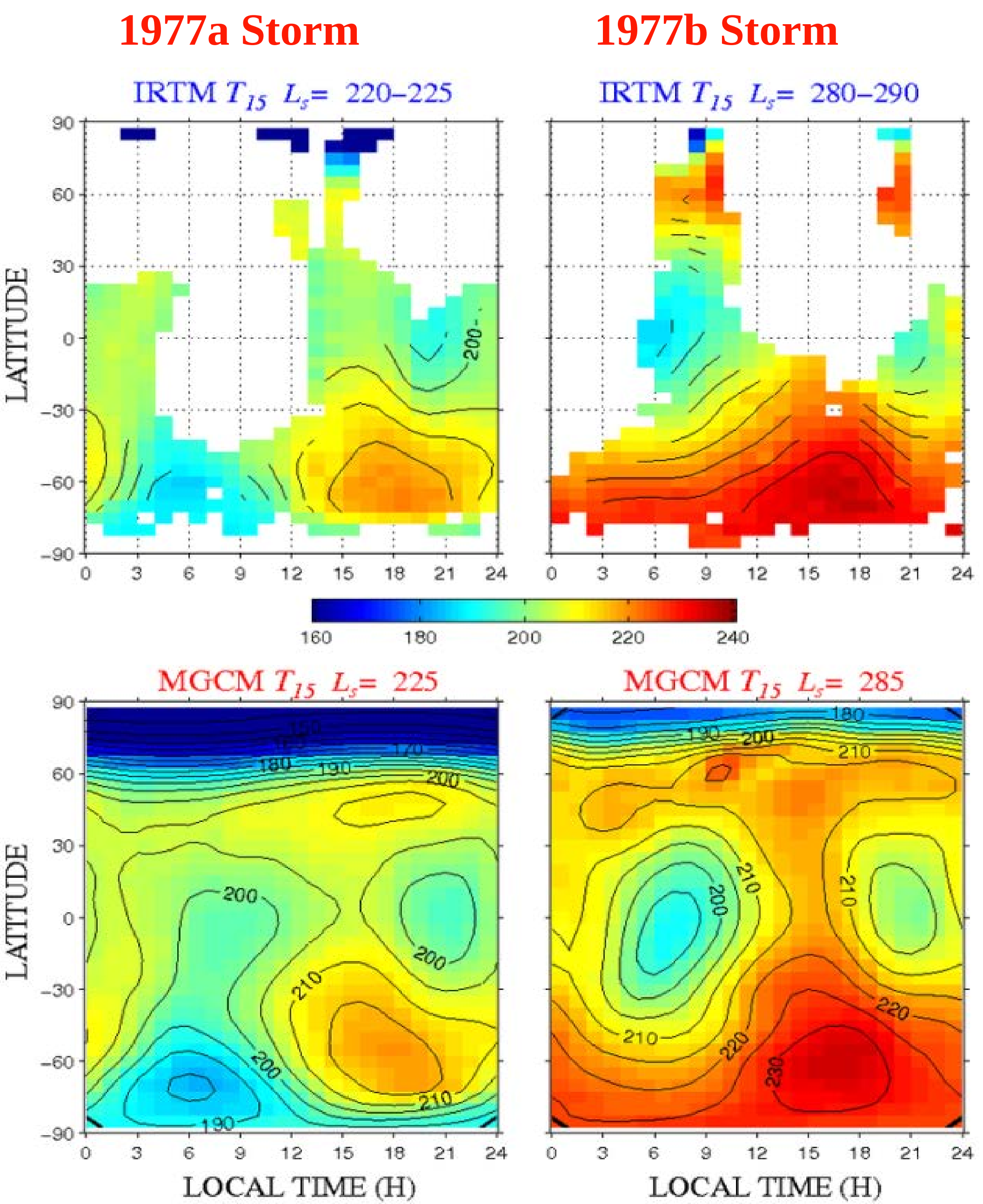

Viking IRTM

T_{15} (0.5 hPa or ~ 25 km)

Observed

Latitude x Local Time

Simulated (MGCM)

binned in local time and zonally averaged

Viking Dust Storm Simulations

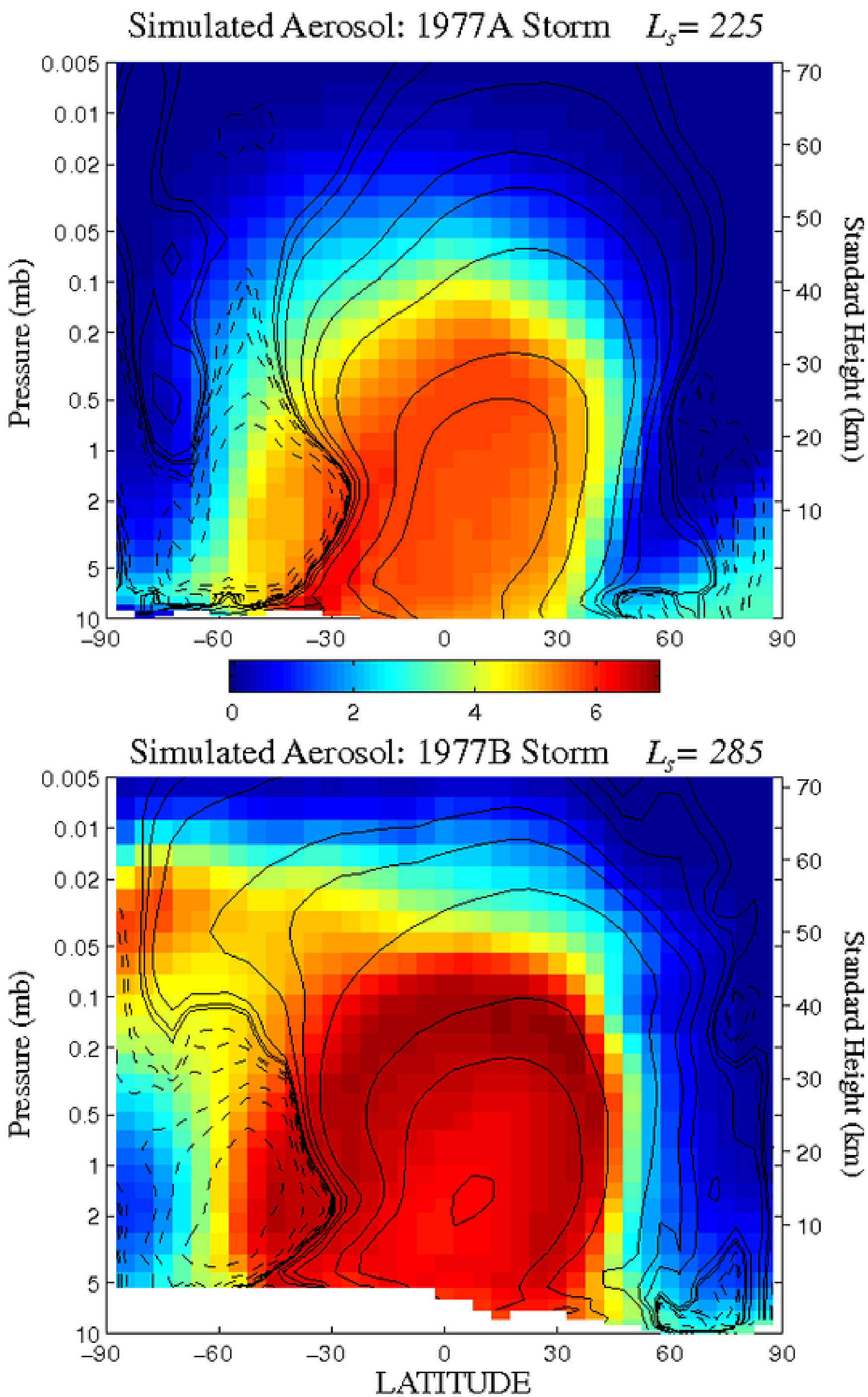

Dust distribution is shaped by the Hadley circulation

Global distribution

Simulated and Observed $S_1(T_{15})$ and $S_2(T_{15})$ Tide Amplitudes for 1977a and 1977b Dust Storms.

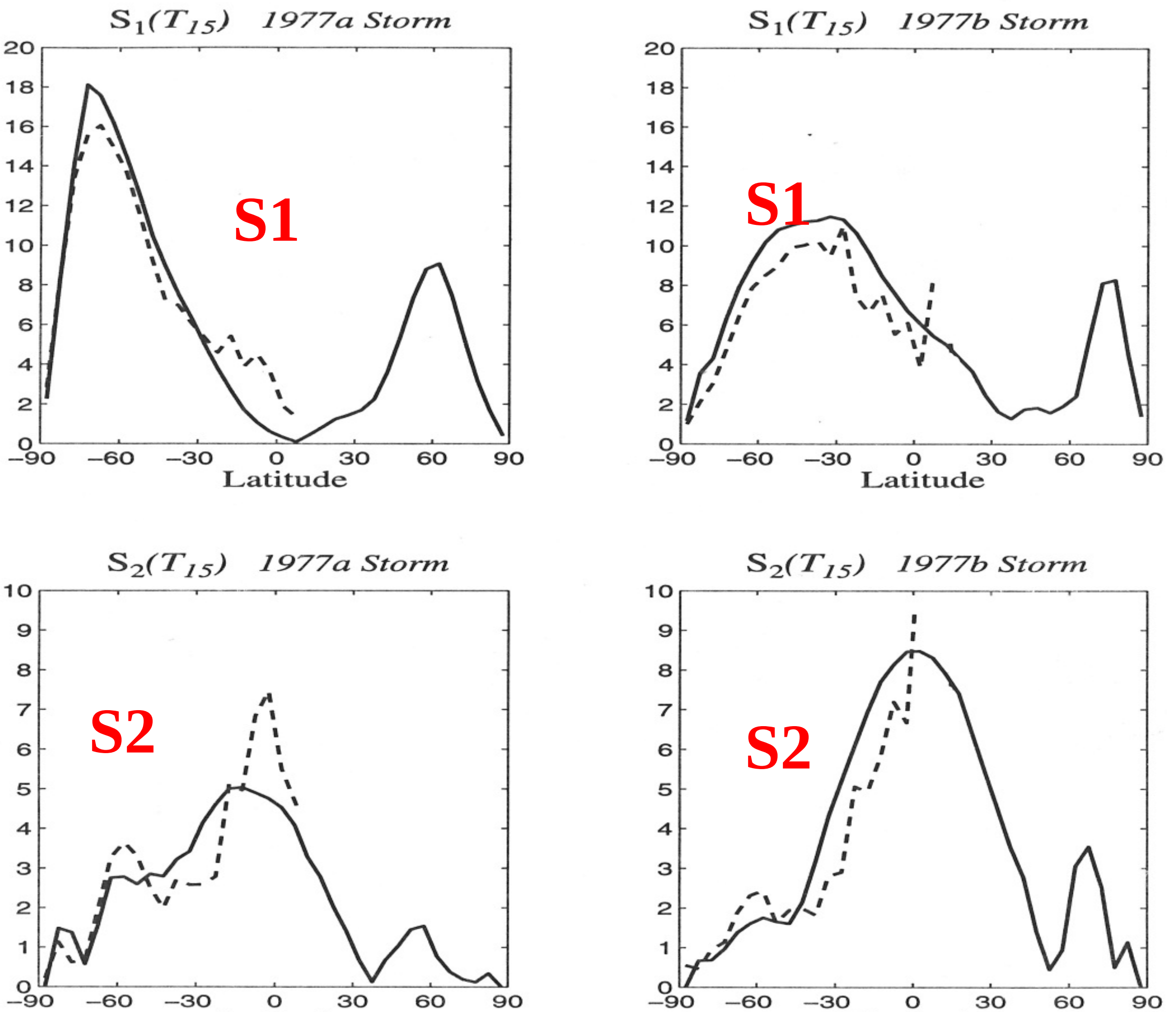

Latitude

Latitude

S_1 stronger in 1977a than 1977b, and at a higher latitude: consistent with the influence of zonal mean westerlies at Ls=225 in 1977a.

S_2 stronger for 1977b– Significantly higher dust opacity in the 2'd storm.

$S_2(T_{15})$ 5- 8 K Amplitude

UK Reanalysis: Equatorial Semidiurnal P_{SFC} Amplitude and Dust Opacity

$$S_2(P_{sfc}) \qquad \tau' = 0.3 + 1.6\,\tau$$

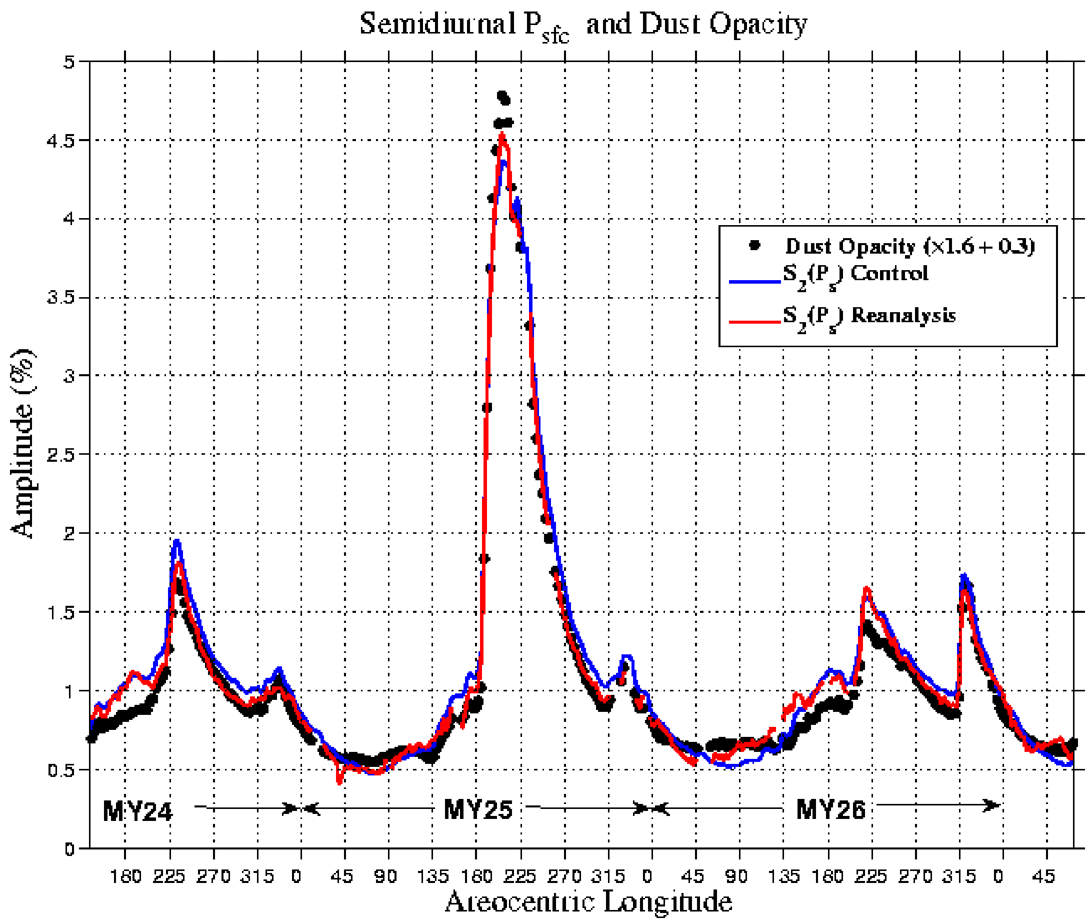

Areocentric Longitude

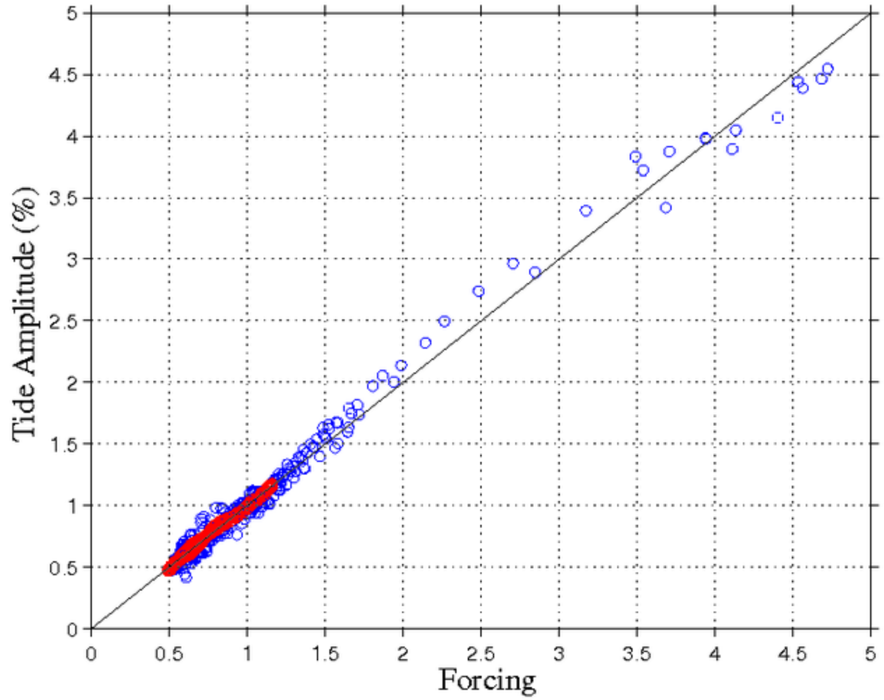

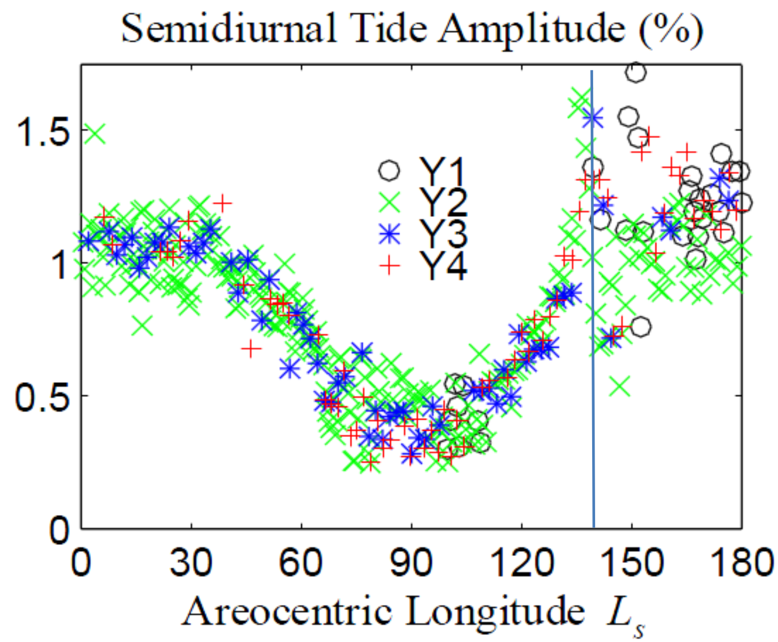

$\mathcal{F} = (\alpha + \beta\tau)\{\cos(\delta)\ R^{-2}\}$ $\alpha = 0.48;$ $\beta = 1.32$

Seasonal variation in equatorial (symmetric) insolation based on orbital radius R and declination δ

α is due to boundary layer heating

$S_2 \sim 1$ ⟹ $\tau \sim 0.5$

MGCM Simulation with Radiatively Active Ice Clouds

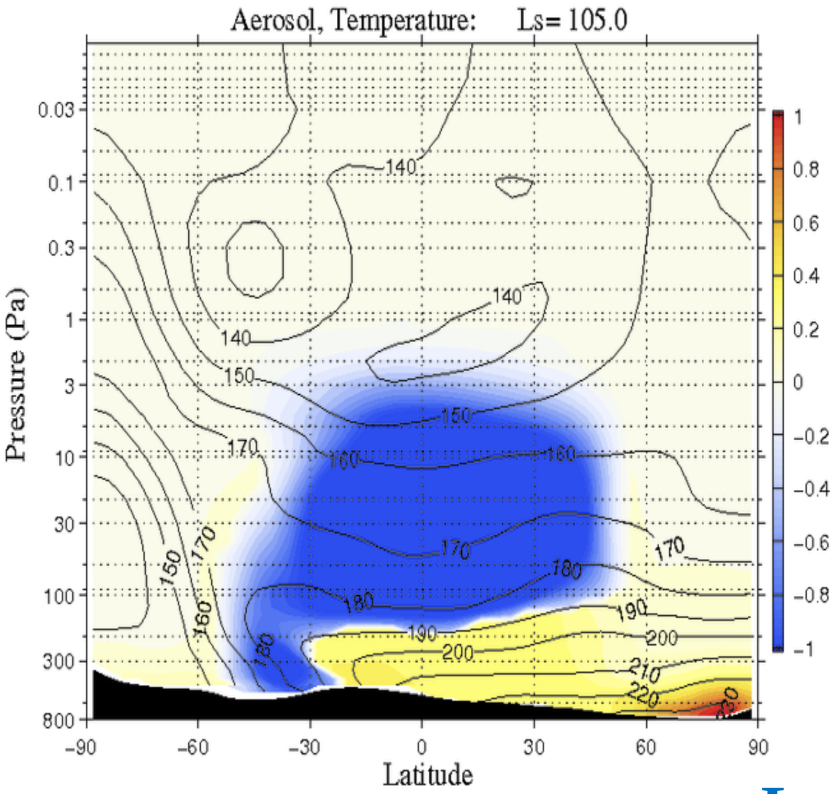

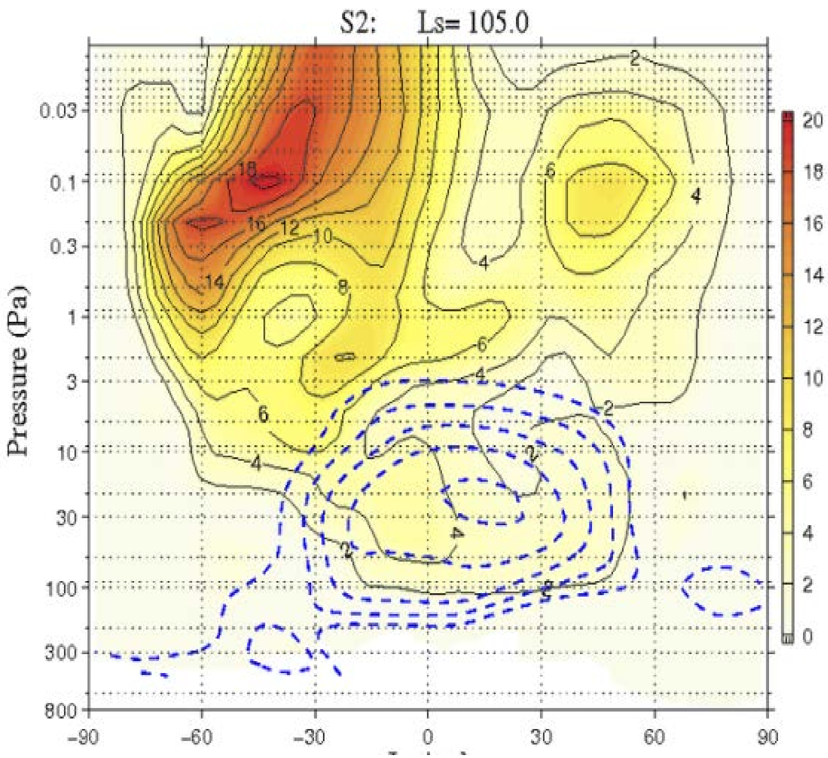

Latitude

Migrating Semidiurnal Tide Amplitude $L_s = 105$

GFDL | **LMD MCD**

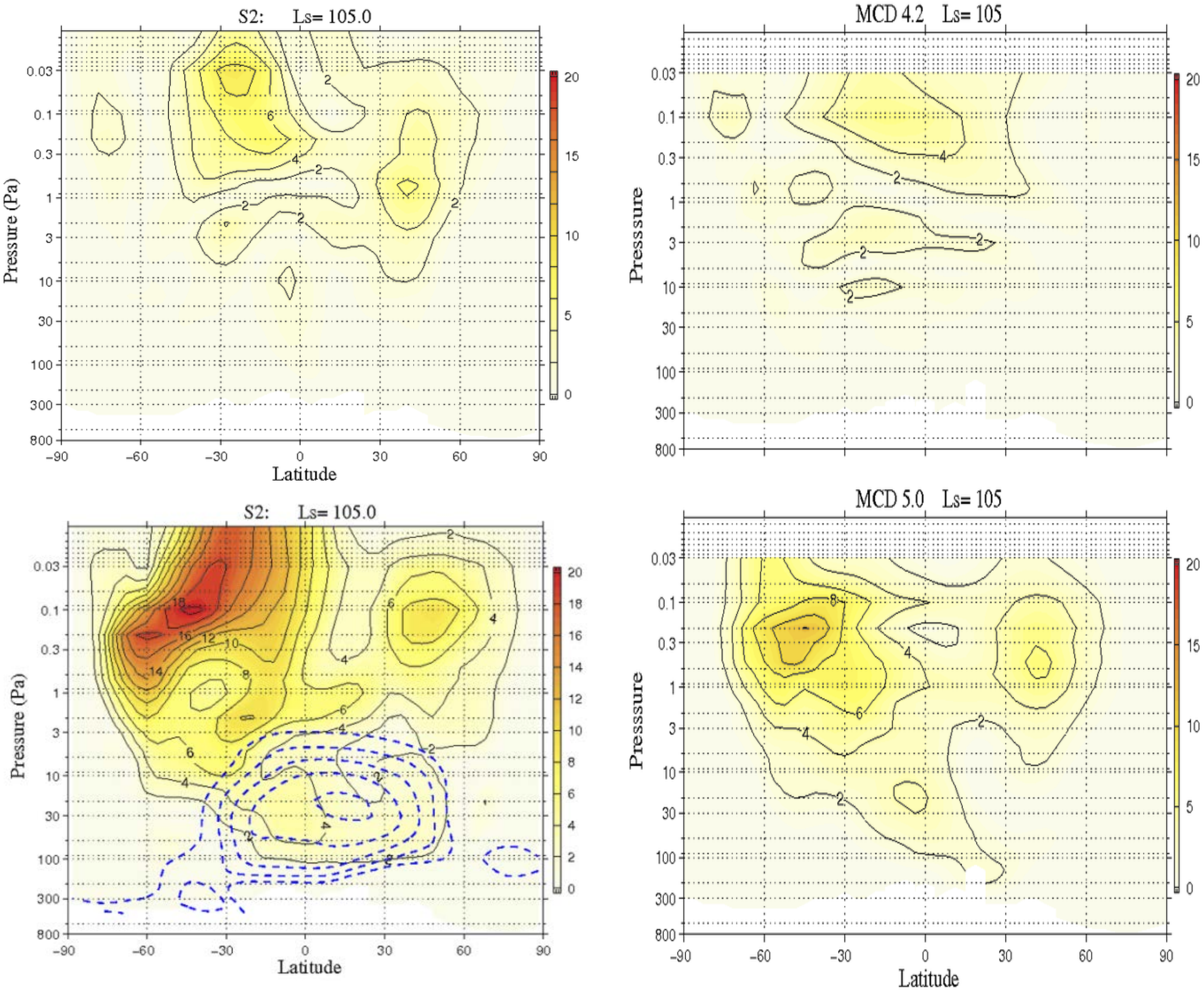

No Clouds

Radiatively Active Water Ice Clouds

Pressure (Pa)

Latitude

Ls 99-113 ave, zonal mean semi-diurnal tide amplitude, T

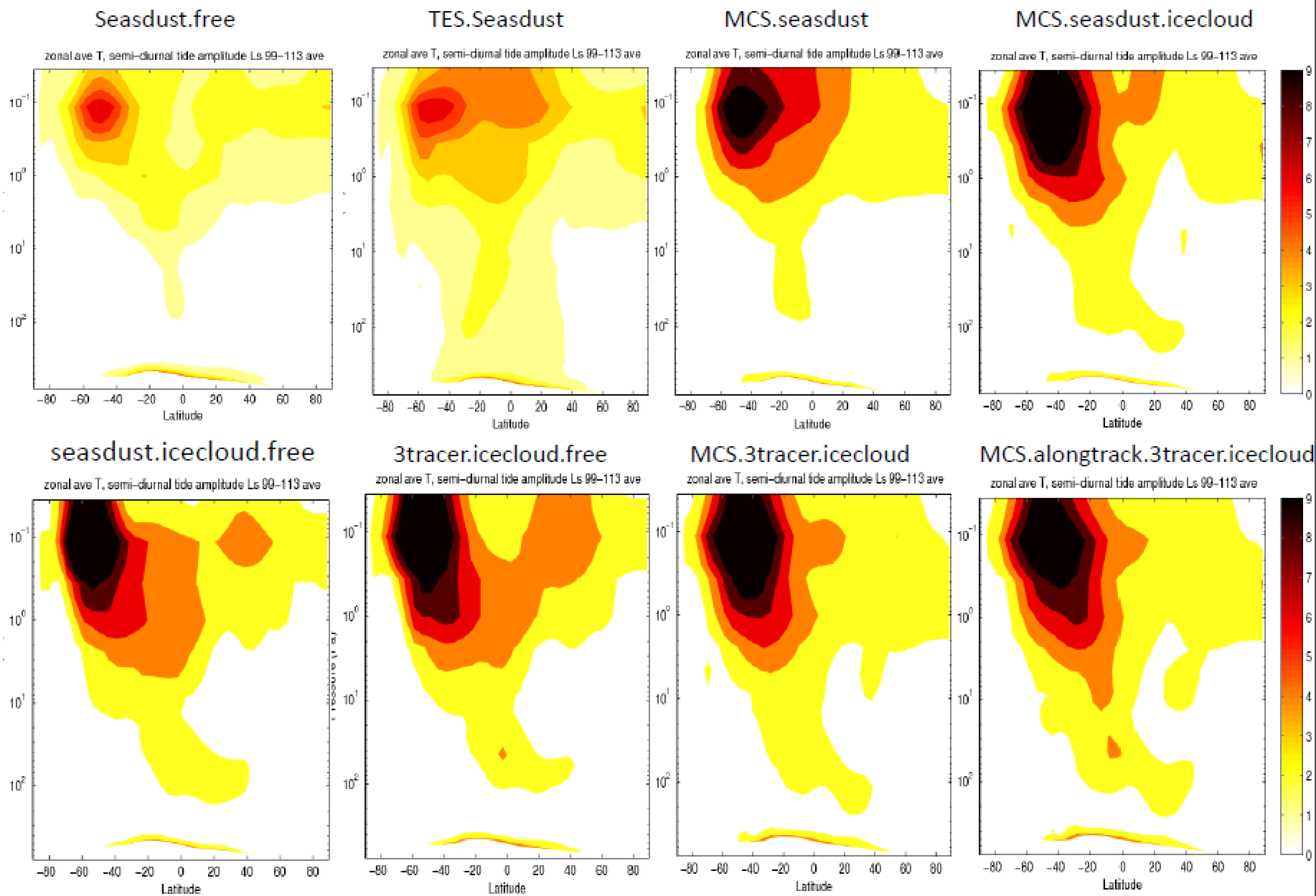

Summary

The evidence for coupling between tropical clouds and the thermal tide first seen in MGS Radio Science observations has been reinforced with the much more extensive and comprehensive data returned from MCS.

•The presence of strong elevated nighttime temperature inversions in the Tharsis region is a robust feature of the equatorial atmosphere during the L_s= 0-140° season, with little difference seen between the two Mars years examined (MY 29 and 30).

•The tropical structure appears to evolve over the spring and summer seasons in response to the waxing and waning of tropical cloud opacity. MGCM simulations suggest that radiative forcing by water ice clouds plays a significant role in establishing the observed structure.

•The zonal temperature anomalies described here are dominated by tide modes that include eastward propagating, diurnal period Kelvin waves and shorter vertical wavelength westward propagating tide modes.

MCS temperature and cloud observations will provide valuable guidance and constraints for future model development.

•Modeling of 32 micron (~surface) brightness temperature with radiatively active clouds should yield estimates column cloud opacity. MCS retrievals do not provide this observation and retrievals are limited by optically-thick clouds.

•The vertical extent of clouds should be strongly influenced by cloud microphysics